USGS
science for a changing world

Prepared in cooperation with the U.S. Army Corps of Engineers, Portland District

Tracking Heat in the Willamette River System, Oregon

Scientific Investigations Report 2022–5006

U.S. Department of the Interior
U.S. Geological Survey

Cover. Willamette River near Harrisburg, Oregon, as seen looking upstream toward the Harrisburg Bridge, Oregon. Photograph taken by Rose Wallick, U.S. Geological Survey, June 27, 2021.

Tracking Heat in the Willamette River System, Oregon

By Stewart A. Rounds and Laurel E. Stratton Garvin

Prepared in cooperation with the U.S. Army Corps of Engineers, Portland District

Scientific Investigations Report 2022–5006

U.S. Geological Survey, Reston, Virginia: 2022

Suggested citation:
Rounds, S.A., and Stratton Garvin, L.E., 2022, Tracking heat in the Willamette River system, Oregon: U.S. Geological Survey Scientific Investigations Report 2022–5006, 47 p., https://doi.org/10.3133/sir20225006.

Associated data for this publication:
Stratton Garvin, L.E., and Rounds, S.A., 2022, CE-QUAL-W2 models for the Willamette River and major tributaries below U.S. Army Corps of Engineers dams—2011, 2015, and 2016: U.S. Geological Survey data release, https://doi.org/10.5066/P908DXKH.

ISSN 2328-0328 (online)

Contents

Figures

Tables

Conversion Factors

U.S. customary units to International System of Units

Multiply	By	To obtain
foot (ft)	0.3048	meter (m)
mile (mi)	1.609	kilometer (km)
square mile (mi^2)	2.590	square kilometer (km^2)
acre-foot (acre-ft)	1,233	cubic meter (m^3)
cubic foot (ft^3)	0.02832	cubic meter (m^3)
cubic foot per second (ft^3/s)	0.02832	cubic meter per second (m^3/s)
mile per hour (mi/h)	1.609	kilometer per hour (km/h)

International System of Units to U.S. customary units

Multiply	By	To obtain
meter (m)	3.281	foot (ft)
kilometer (km)	0.6214	mile (mi)
square kilometer (km^2)	0.3861	square mile (mi^2)
cubic meter (m^3)	0.0008107	acre-foot (acre-ft)
cubic meter (m^3)	35.31	cubic foot (ft^3)
cubic meter per second (m^3/s)	35.31	cubic foot per second (ft^3/s)
kilometer per hour (km/h)	0.6214	mile per hour (mi/h)

Temperature in degrees Celsius (°C) may be converted to degrees Fahrenheit (°F) as follows:

$$°F = (1.8 \times °C) + 32.$$

Temperature in degrees Fahrenheit (°F) may be converted to degrees Celsius (°C) as follows:

$$°C = (°F - 32) / 1.8.$$

Datums

Vertical coordinate information is referenced to the North American Vertical Datum of 1988 (NAVD 88).

Horizontal coordinate information is referenced to the North American Datum of 1983 (NAD 83).

Supplemental Information

The models and the results of model simulations developed and used in this study are available on Science Base at https://doi.org/10.5066/P908DXKH.

Abbreviations

7dADMean	7-day average of the daily mean
BCL	Big Cliff Dam
BLU	Blue River Dam
CE-QUAL-W2	two-dimensional flow and water-quality model
CGR	Cougar Dam
COT	Cottage Grove Dam
DEX	Dexter Dam
DOR	Dorena Dam
EEF	environmental energy flux
EEFR	ratio of incoming to outgoing environmental energy fluxes across water surface
FAL	Fall Creek Dam
FOS	Foster Dam
HRTS	heat replacement time scale
USACE	U.S. Army Corps of Engineers
USGS	U.S. Geological Survey
WVP	Willamette Valley Project

Tracking Heat in the Willamette River System, Oregon

By Stewart A. Rounds and Laurel E. Stratton Garvin

Abstract

The Willamette River Basin in northwestern Oregon is home to several cold-water fish species whose habitat has been altered by the Willamette Valley Project, a system of 13 dams and reservoirs operated by the U.S. Army Corps of Engineers. Water-resource managers use a variety of flow- and temperature-management strategies to ameliorate the effects of upstream Willamette Valley Project dams on the habitat and viability of these anadromous and native fish. In this study, new capabilities were added to the CE-QUAL-W2 two-dimensional flow and water-quality model to inform those flow- and temperature-management strategies by tracking the quantities and ages of water and heat from individual upstream sources to downstream locations in the Willamette River system. Specifically, the fraction of water and heat attributable to upstream dam releases or other water inputs, and the fraction of heat sourced from environmental heat fluxes across the water and sediment surfaces, were tracked and quantified in the river at all locations and times simulated by the model. Applying the updated CE-QUAL-W2 models to the Willamette River system for the months of March through October in the years 2011 (cool and wet), 2015 (hot and dry), and 2016 (warm and somewhat dry) demonstrated that the influence of upstream dam releases on downstream water temperature diminished within a few days as water moved downstream. At sites that are roughly two or more days of travel from upstream dams (Albany and downstream), the July–August fraction of riverine heat content that could be tracked back to upstream dam releases typically diminished to less than 20 percent, despite the fact that roughly 50 percent of July–August streamflow could be attributed to upstream dam releases at the same sites. In contrast, the fraction of riverine heat content that could be attributed to environmental energy fluxes continued to increase with downstream distance, from about 59 to 67 percent at Albany during July–August to 62 to 73 percent at Keizer and 68 to 79 percent at Newberg.

At locations sufficiently far downstream, upstream dam releases affect water temperature mainly through a decrease in travel time (less time for environmental heat fluxes to warm the river during summer) and an increase in thermal mass (more water to dilute and buffer incoming heat fluxes) rather than through the simple transport of heat content (water temperature) released from the dams. This concept was explored not only for the baseline conditions that occurred in March–October of 2011, 2015, and 2016, but also for a hypothetical high-flow release during August 2016 and an actual high-flow release during August 2017. In these high-flow releases, an extra 2,500 cubic feet per second (roughly) was released from Dexter Dam on the Middle Fork Willamette River, and downstream effects were measured (2017, actual) and simulated (2016, hypothetical). Results of the simulations were consistent with insights gained from the baseline conditions, such that temperature changes caused by flow augmentation were substantial in upstream reaches (measured cooling of about 1.5 °C near Harrisburg [43 miles downstream] and Albany [84 miles downstream] in 2017, and cooling of about 0.5 °C near Albany in 2016) and diminished farther downstream, but still measurable (more than a few tenths of a degree Celsius) even at Newberg, which is about 154 miles downstream. The direct downstream effects of dam releases on the river heat content attributable to those releases were increased by the hypothetical flow augmentation, with increases of 20 percent at Harrisburg and 12 percent at Keizer. Even with a decreased influence of environmental energy fluxes on river heat content, however, the fraction of heat content attributable to such fluxes was still more than 50 percent at and downstream of Albany and more than 70 percent at Newberg, where the river temperature was less affected by upstream dam-release temperatures and instead was affected primarily by a decreased travel time and increased thermal mass.

Heat transport processes and energy fluxes across the river surface also were quantified and examined to produce several informative time scales, ratios, and dimensionless numbers that may help water-resource managers to better understand the extent to which upstream dam releases affect downstream water temperatures. The Heat Replacement Time Scale (HRTS), for example, was defined as the ratio of the heat content of water in the river at a particular location divided by the incoming environmental energy flux across the water surface—essentially the time it would take to replace the existing heat content with incoming environmental energy fluxes. The HRTS increases with depth because a deeper river reach with the same surface area and temperature has more water volume and a greater heat content. The HRTS in the Willamette River often was less than 5 days at most locations upstream of Newberg during summer; the river is deeper downstream of Newberg, resulting in a larger HRTS. Given a typical late-summer travel time of 2–4 days from upstream dams to the reach between Albany and Newberg, an HRTS of less than 5 days is consistent with a diminished heat content attributable to upstream dam releases. Other metrics that were

explored include the ratio of advective heat flux to incoming environmental energy flux and the ratio of incoming to outgoing environmental energy fluxes across the water surface. These analyses and results should not only help water-resource managers better formulate flow- and temperature-management strategies, but also help them create better strategies that are based on stream heat budgets and the known dynamics of the Willamette River system.

Introduction

The Willamette River Basin in northwestern Oregon (fig. 1) is home to several formerly abundant populations of cold-water-adapted salmonids, including spring-run Chinook salmon (*Oncorhynchus tshawytscha*) and winter-run steelhead (*O. mykiss*). After more than a century of decline caused by pollution, overfishing, habitat loss, habitat degradation, and other factors, these populations were listed as threatened in 1999 under the Endangered Species Act (ESA) of 1973 (Public Law 93–205, 87 Stat. 884, as amended) (National Marine Fisheries Service, 2008). Among the challenges to the health and survival of these salmonids, thermal conditions are a major factor (National Marine Fisheries Service, 2008; Oregon Department of Fish and Wildlife and National Marine Fisheries Service, 2011). Changes to the thermal regime of the Willamette River and its tributaries have been shown to affect egg survival, emergence, smoltification and out-migration of juveniles, prespawn mortality, and rates of predation and disease (McCullough, 1999; Caissie, 2006; Keefer and others, 2010; Olden and Naiman, 2010; Perry and others, 2015).

The thermal regime of the Willamette River and its tributaries is affected by two related but distinct anthropogenic effects—a disruption or shift away from a "natural" seasonal temperature pattern, particularly in the tributaries, and an aggravation of maximum temperatures farther downstream. Thirteen large, multi-purpose dams operated by the U.S. Army Corps of Engineers (USACE) and located on major tributaries of the Willamette River influence the seasonal patterns and magnitude of variation in streamflow and water temperature downstream of the dams (Rounds, 2010). Together with a series of revetments, fish hatcheries, and other installations, these 13 dams constitute the Willamette Valley Project (WVP), which the USACE operates to provide flood-risk management, irrigation, navigation, hydropower, fish and wildlife benefits, water-quality benefits, recreation, and water supply (U.S. Army Corps of Engineers, 2019). The height, outflow structures, storage capacity, and operations of each dam are unique; however, all of the WVP dams alter the thermal regimes of the waterways downstream. The size and thermal stratification of the impounded reservoirs and the uniformity of some dam operations causes the WVP dams to buffer temperatures downstream, moderating both diurnal and annual variability and retarding the annual warming and cooling cycles (Lowney, 2000; Steel and Lange, 2007; Olden and Naiman, 2010). Rounds (2010) showed that the annual temperature maximum immediately downstream of tall dams in the Willamette River Basin tended to be delayed by about a month and that release temperatures could be 6 to 10 °C warmer or cooler compared to a no-dams condition.

In addition to seasonal lags in temperature patterns caused by large dams on its tributaries, the Willamette River routinely exceeds regulatory criteria for maximum stream temperature, thereby exposing threatened salmonid populations to adversely warm conditions in summer and autumn (Stratton Garvin and Rounds, 2022a; Stratton Garvin and others, 2022b). In a Total Maximum Daily Load analysis, anthropogenic influences such as degraded riparian vegetation and point-source discharges were determined to exacerbate these warm conditions (Oregon Department of Environmental Quality, 2006; Rounds, 2007). The State of Oregon has set maximum water-temperature criteria (18 or 20 °C during summer, depending on the reach-designated fish use) for certain reaches of the Willamette River to help protect temperature-sensitive fishes (Oregon Department of Environmental Quality, 2003, 2005, and 2016). In a climatological analysis based on measured temperatures in the Willamette River, Stratton Garvin and others (2022b) showed that in a median hydrologic and climatic year, the 7-day averages of the daily mean and the daily maximum water temperature of the Willamette River are likely to exceed 18 °C in July at least as far upstream as Harrisburg, comprising more than 110 miles of river designated by the 18 °C regulatory criterion upstream of Newberg. In 2014, the hottest July through September period on record in the Willamette Valley (Costanzo and others, 2015; NOAA National Centers for Environmental information, 2020), six continuous temperature monitors in the Willamette River reported 7-day averages of the daily maximum water temperature exceeding the state regulatory criterion between 77 and 83 percent of summer days.

To address temperature issues both near the dams and farther downstream in the Willamette River, USACE has relied on a multi-pronged approach. First, where possible, dam releases have been managed to approach a more-natural seasonal temperature pattern by releasing water from different depths in reservoirs that thermally stratify during summer. This strategy has been implemented at several dams through operational changes and the use of existing dam outlets (at Detroit Dam, for example; see Buccola and others, 2012) and implemented or planned at other dams by building a selective withdrawal tower to allow the custom blending of water from different depths and temperatures to meet a downstream temperature target (Rounds, 2007; Buccola and others, 2015). Second, to limit peak temperatures in the Willamette River, flow augmentation from reservoir storage is used to increase summer streamflow at Albany and Salem to about double the pre-dam average flow (National Marine Fisheries Service, 2008; Rounds, 2010). Higher streamflow during summer can limit maximum temperatures by buffering the temperature response of the river to environmental heat loads and by increasing the stream velocity, which reduces the time that water is exposed to environmental heat fluxes as it travels downstream.

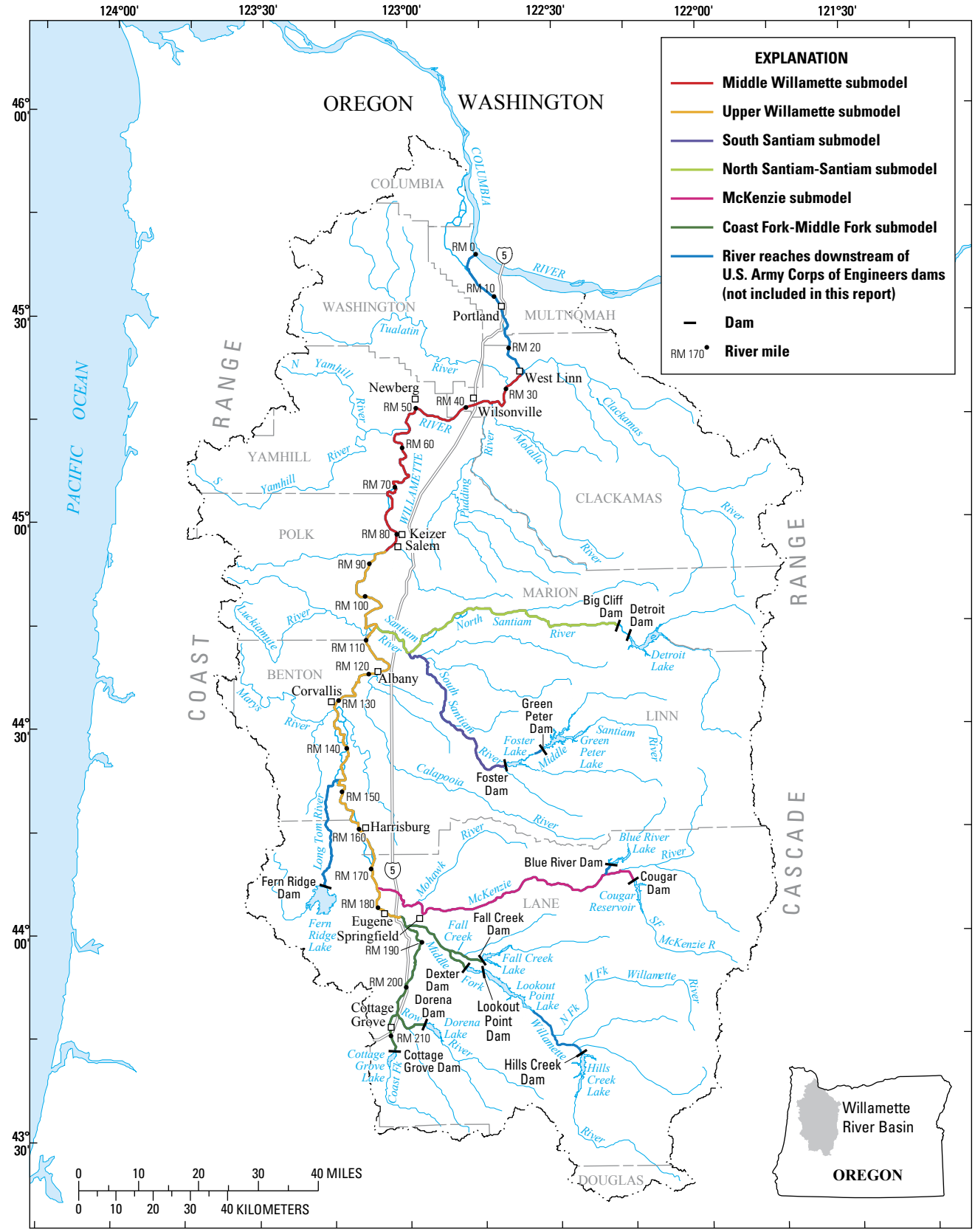

Base map modified from U.S. Geological Survey and other digital data sets (1:2,000,000; 1:100,000). Projection: Oregon Lambert Conformal Conic, NAD1983, NAVD1988.

Figure 1. Willamette River Basin in northwestern Oregon, showing the Willamette Valley Project dams and reservoirs and the main river reaches modeled in this study. Map modified from Stratton Garvin and others (2022a).

The interplay of these two management strategies, and the downstream distance over which direct temperature management of dam releases may be influential, however, has not been fully understood or quantified. Stream temperature is constantly in flux, warming or cooling toward an ever-changing, meteorologically controlled "equilibrium temperature" at which the net flux of heat across the air/water interface is zero (Edinger and others, 1968; Bogan and others, 2003). The rate of heat exchange between the river and the atmosphere is a function of short-wave solar radiation, long-wave atmospheric radiation and back radiation, evaporation, and conductive heat transfer between the air and water (Edinger and others, 1968). The temperature of water in a given stream reach, then, is a function of the temperature of the water flowing from upstream and other hydrologic inputs (such as tributaries), the volume and surface area of the stream, the rate of heat exchange with the atmosphere, and the rate of heat exchange with sediments (less important in large rivers). The persistence of a heat signature originating upstream, such as that from a dam release, thus depends on how quickly that upstream-sourced heat is replaced by heat exchanged with the atmosphere, the amount of upstream-sourced heat to be replaced, and the velocity of the stream, which controls the distance traveled while the temperature adjusts. Estimates of the distance required for "thermal recovery" from dam releases typically range from about 25 miles to more than 500 miles, depending on the river system, as different rivers may have widely varying channel characteristics and velocities (Ward, 1985; Palmer and O'Keefe, 1989; Stevens and others, 1997; Preece and Jones, 2002).

Rounds (2010) showed that the thermal effect of dams in the Willamette River system decreased to a seasonally dependent difference of 1–2 °C downstream of the confluence of the Santiam River with the Willamette River (about 50 river miles downstream from the nearest WVP dam). This estimate, however, was based on the modeled difference between a regulated versus free-flowing temperature regime and did not differentiate between the direct thermal influence of dams and the cooling effect of summer flow augmentation on the Willamette River. Similarly, most previous research efforts to quantify the downstream distance of a dam's influence on temperature have relied on a combination of historical data and modeling to compare stream temperatures under free-flowing versus regulated flow conditions (for example, Palmer and O'Keefe, 1989; Preece and Jones, 2002; Arora and others, 2018).

Stream Temperature Controls

The heat content and water temperature of a stream are controlled by the inputs and outputs of heat to and from that stream, including heat that enters or leaves with the flow of water (advected heat) as well as energy that enters or leaves the stream across the air/water or sediment/water interface. The environmental energy flux (EEF) across the air/water and sediment/water interfaces is an important influence on the temperature of most streams (Edinger and others, 1968). The components of the EEF are depicted in figure 2 and the net EEF may be defined as (Wells, 2019):

$$H_n = (H_s - H_{sr}) + H_a - H_b - H_e - H_c \quad (1)$$

where

H_n is the net incoming (positive) or outgoing (negative) environmental energy flux across the air/water and sediment/water interfaces,

H_s is the incident energy flux from short-wave solar radiation,

H_{sr} is the reflected energy flux of short-wave solar radiation,

H_a is the incoming energy flux from long-wave atmospheric radiation,

H_b is the outgoing energy flux from long-wave back radiation,

H_e is the outgoing energy flux caused by evaporation (when positive) or the incoming energy flux caused by condensation (when negative), and

H_c is the outgoing (positive) or incoming (negative) energy flux from conduction across the air/water and sediment/water interfaces.

Solar radiation is the energy from sunlight, some of which may be prevented from reaching the water surface by shade from surrounding topography or nearby vegetation and some of which may be reflected upon reaching the water surface. The terms "short-wave" and "long-wave" denote relative wavelengths, where "short-wave" refers to wavelengths in the ultraviolet, visible, and near-infrared that comprise solar radiation, and "long-wave" refers to longer wavelengths in the infrared that comprise blackbody radiation from the atmosphere or the river surface. The evaporative energy flux accounts for the energy required to change some mass of liquid water to water vapor when that water evaporates from the river surface, and that energy flux can be negative (added to the stream) if condensation rather than evaporation occurs. The conductive energy flux accounts for heat moving across the air/water or sediment/water interface simply because the water is in direct contact with a medium (air or sediment) that may have a different temperature.

The largest components of the EEF over the course of a day typically are long-wave back radiation from the water surface and long-wave atmospheric radiation, when these fluxes are considered separately (Edinger and others, 1968; Brown, 1969). During a sunny day with minimal shade, short-wave solar radiation also contributes a large energy flux, but typically less than the daily total energy flux of long-wave atmospheric radiation. Evaporative heat losses on warm sunny days tend to be substantial, but less than losses from back radiation. In large and relatively deep rivers, energy fluxes from conduction typically are the smallest, relative to the others mentioned, but conduction of energy to stream sediments can be more important in small shallow streams (Brown, 1969; Sinokrot and Stefan, 1993).

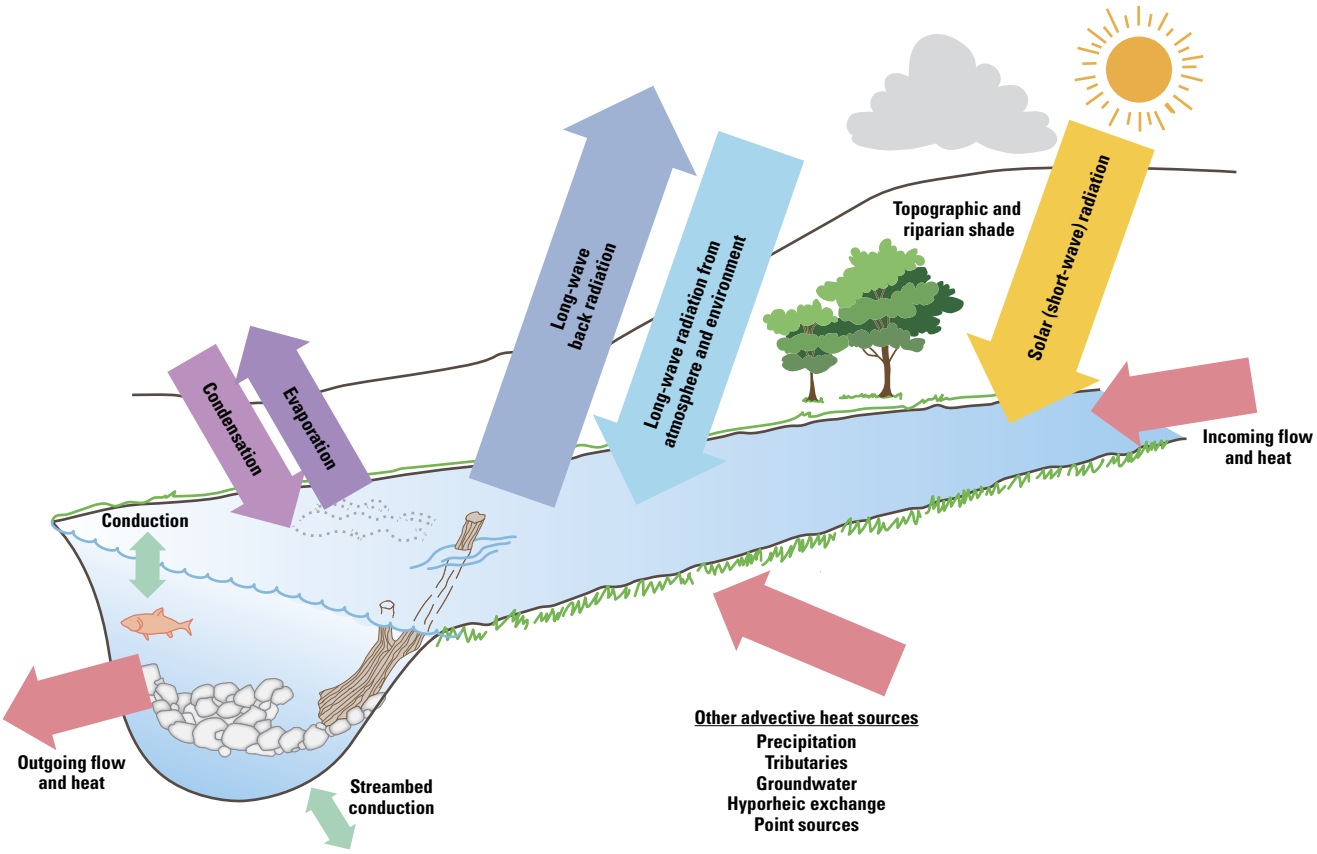

Figure 2. Heat fluxes that affect water temperature in a stream, including advective fluxes that import or export heat with the flow of water and the energy fluxes that occur at the air/water and sediment/water interfaces. Figure adapted from Bartholow (2000).

Water temperature in a stream changes in response to advective heat fluxes as well as the EEFs across the air/water and sediment/water interfaces, and water temperature is buffered by the heat capacity, or thermal mass, of the waterbody. Advective heat fluxes include the addition, removal, or movement of heat from tributary or point-source inflows, groundwater discharge or recharge, hyporheic flows, and the surface-water flow of the waterbody itself (fig. 2). The advective heat flux depends on the amount of flow and the temperature of the moving water. In large rivers such as the Willamette River, the advective heat flux of the river itself can be much larger than the daily EEFs.

Finally, shading of solar radiation and the physical dimensions of a waterbody are important to the heat budget of a waterbody (Edinger and others, 1968; Wells, 2019). Topographic and vegetative shade can greatly decrease the incoming energy flux from solar radiation, which is particularly important to a stream heat budget in summer when days are long and solar radiation is intense. The total amount of energy moving across the air/water interface depends on the width of the waterbody, with wide streams capturing and releasing larger amounts of energy than narrow streams. In deep waterbodies, more water is present to buffer temperature changes caused by EEFs and advective heat inflows. Therefore, the width-to-depth ratio of a stream is a critical determining factor for its susceptibility to changes in temperature, with wide, shallow streams having greater daily temperature variations and less ability to buffer against changes in temperature than narrow, deep streams.

Study Area

The Willamette River Basin in northwestern Oregon comprises approximately 11,500 mi^2, bounded by the Cascade Range to the east and south, the Coast Range to the west, and the Columbia River to the north (fig. 1). The climate is classified as warm-summer Mediterranean, with cool, wet winters and warm, dry summers; most precipitation falls as rain in the lowlands and snow in the upper elevations of the Coast and Cascade Ranges (Kottek and others, 2006). Peak flows in the Willamette River, the principal river draining the basin, tend to occur during winter storms, whereas flows are typically low and stable in the summer and early autumn. Except where influenced by dam releases, stream temperatures in the Willamette River system generally follow seasonal air-temperature patterns, with annual minima occurring in early January and annual maxima in late July or early August (Stratton Garvin and Rounds, 2022a).

The Willamette River Basin is home to 70 percent of Oregon's population and most of its major metropolitan areas, including the cities of Portland, Salem, Corvallis, Albany, Eugene, and Springfield (Rounds, 2010). Flood-risk hazard mitigation in the basin is provided by the WVP, a system of 13 dams and other installations first authorized in 1938 (National Marine Fisheries Service, 2008). The 13 reservoirs in the WVP can store up to about 1.6 million acre-ft of water to fulfill various downstream uses (U.S. Army Corps of Engineers, 2019). The dams range in height and storage capacity but each is operated to a "rule curve," a reservoir-specific operational water-control diagram that specifies the target water-surface elevation behind each dam throughout the year. In general, WVP reservoirs authorized for flood-risk management are filled in springtime, then drawn down by tens to hundreds of meters in late summer and autumn to create storage space for inflows from large winter storms. The stored water is allocated for agricultural irrigation, municipal and industrial supply, and maintenance of fish and wildlife habitat (U.S. Army Corps of Engineers, 2019). Releases for the benefit of fish and wildlife generally take the form of flow augmentation during spring through late summer to improve downstream aquatic habitats and water quality. River managers from USACE follow detailed operational rules for each dam and reservoir, use a set of time-varying flow targets for critical downstream river locations, and apply models that help them plan and carry out releases to meet their goals for reservoir water storage and river flow management.

Purpose and Scope

This study, carried out by the U.S. Geological Survey (USGS) in partnership with the USACE, uses a novel, model-based tracer approach to gain insights into the thermal patterns in a river network and determine the extent to which upstream sources of water and upstream release temperatures can be expected to influence downstream temperatures. The primary purpose of this study was to develop new algorithms for the CE-QUAL-W2 flow and water-quality model (Wells, 2019) and use those new capabilities to track water, heat, and the ages of water and heat from specific sources through a river system. The Willamette River system in northwestern Oregon was used as a case study to increase our understanding of heat sources to the Willamette River and the sensitivity of water temperature at downstream locations to the amount and temperature of upstream dam releases. A secondary purpose of the study was to develop a better understanding of riverine heat budgets and heat fluxes, again using the Willamette River as a case study, and to develop new ways of thinking about and quantifying those heat fluxes. This report reflects the purposes of the overall study in that it (1) describes and documents the newly developed water- and heat-tracking capabilities that were added to the CE-QUAL-W2 model, (2) quantifies the amount of water and heat contributed by various sources to the Willamette River system over space and time, (3) introduces several time scales, ratios, and dimensionless numbers that might provide useful insights into riverine energy fluxes and heat transport, and (4) describes the implications of these water- and heat-source analyses on flow- and temperature-management strategies, including flow augmentation, in the Willamette River system.

The spatial scope of this study includes the Willamette River upstream of Willamette Falls and most of its major regulated tributaries from the Willamette River up to the first major dam (fig. 1). In the Santiam River subbasin, these tributaries include the Santiam River, the South Santiam River up to Foster Dam, and the North Santiam River up to Big Cliff Dam. In the McKenzie River subbasin, the models include the McKenzie River upstream to the mouth of the South Fork McKenzie River and then upstream along the South Fork McKenzie River to Cougar Dam. In the Middle Fork Willamette River subbasin, the models include the Middle Fork Willamette River up to Dexter Dam and Fall Creek up to Fall Creek Dam. In the Coast Fork Willamette River subbasin, the models include the Coast Fork Willamette River upstream to Cottage Grove Dam, and the Row River upstream to Dorena Dam. Other tributaries are handled as point inputs.

All of the models were developed for previous studies and updated for conditions that occurred from late March through the end of October for 2011, 2015, and 2016 (Stratton Garvin and others, 2022a), which are the time periods for this study. These three years represent a range of conditions, where 2011 was "cool and wet" with higher-than-average streamflows and generally cool water temperatures and 2015 was "hot and dry" with lower-than-average streamflows and warm weather, particularly in June of 2015. The conditions that occurred in 2016 were more representative of typical conditions that occur in western Oregon during spring through early autumn in a not extreme, but relatively warm and dry year. These recent years also are representative for the operational rules and flow-management strategies that have been used by USACE largely since 2001 (National Marine Fisheries Service, 2008) and since temperature-management strategies have been introduced at key upstream dams (2007 at Detroit Dam on the North Santiam River and 2005 at Cougar Dam on the South Fork McKenzie River).

Study Methods

Simulation of Flow and Water Quality: CE-QUAL-W2 Model

CE-QUAL-W2 is a two-dimensional (longitudinal, vertical) mechanistic model that simulates water level, flow, water temperature, and many water-quality constituents. The model has been applied successfully to hundreds of waterbodies around the world (Wells, 2019), including many studies of water temperature in the rivers and reservoirs of the Willamette River Basin (Sullivan and Rounds, 2004;

Sullivan and others, 2007; Rounds, 2007; Rounds, 2010; Buccola and others, 2013; Buccola and others, 2016; Buccola, 2017). The CE-QUAL-W2 model is based on equations that describe the conservation of mass, momentum, and energy, with mass movement largely the result of a balance among gravitational and frictional forces, wind shear, and buoyancy. The model includes a full term-by-term representation of heat fluxes across the air/water and sediment/water interfaces and dynamic shading from topography and vegetation, and includes algorithms that allow users to optimize the use of available dam outlets to meet release temperature targets (Wells, 2019; Rounds and Buccola, 2015).

Models Used

Six previously developed and calibrated CE-QUAL-W2 models of various river reaches in the Willamette River stream network were used in this study. These models were built to simulate conditions in the main channel of the river network; side channels and alcoves generally were not included in these laterally averaged models, although the bathymetry used in the models generally accounts for water in any side channels. The six models have been documented by Stratton Garvin and others (2022a) and include the following river reaches delineated in figure 1:

1. South Fork McKenzie River from Cougar Dam (CGR) to its confluence with the McKenzie River, and the McKenzie River downstream from that point to its mouth at the Willamette River. The model includes the Leaburg and Walterville Canals (on the McKenzie River) as model branches as well as Blue River, which is dammed by Blue River Dam (BLU), as a tributary.

2. Middle Fork Willamette River from Dexter Dam (DEX) to its confluence with the Coast Fork Willamette River; Coast Fork Willamette River from Cottage Grove Dam (COT) to its confluence with the Middle Fork Willamette River; Row River from Dorena Dam (DOR) to its confluence with the Coast Fork Willamette River; Fall Creek from Fall Creek Dam (FAL) to its confluence with the Middle Fork Willamette River; and the Willamette River from the Coast and Middle Fork Willamette River confluences to Highway 126 in Springfield.

3. South Santiam River from Foster Dam (FOS) to its confluence with the North Santiam River.

4. North Santiam River from Big Cliff Dam (BCL) to its confluence with the South Santiam River, and the Santiam River from that confluence to its mouth at the Willamette River.

5. Willamette River from Highway 126 in Eugene/Springfield to a location about 1.3 miles upstream of Salem.

6. Willamette River from a location just upstream of Salem to Willamette Falls.

These models were originally constructed and calibrated to support the development of a water-temperature Total Maximum Daily Load for the Willamette River, using data from spring through autumn of 2001 and 2002 (Oregon Department of Environmental Quality, 2006; Annear and others, 2004a and 2004b; Berger and others, 2004; Sullivan and Rounds, 2004; Bloom, 2016).

Since the original development of these river models, the models have been updated and applied for several subsequent uses. Rounds (2007) used the models to evaluate (1) the effects of point sources on river temperature and the effects of trading regulated heat allocations among those point sources, (2) the effects of restoring some riparian vegetation on water temperature, and (3) the effects of revised dam operations at Cougar Dam on downstream temperatures. Later, Rounds (2010) used the models to quantify the downstream thermal effects of all of the WVP dams. More recently, Stratton Garvin and others (2022a) updated the models used in this study to simulate a wide range of more recent conditions, covering spring through autumn of the years 2011 (a cool and wet year), 2015 (a hot and dry year), and 2016 (a warm and somewhat dry year). All of the models used in this study are based on version 4.2 of CE-QUAL-W2 as released by Portland State University on September 20, 2019, with modifications by USGS, and are available to the public at https://doi.org/10.5066/P908DXKH (Stratton Garvin and Rounds, 2022b).

Simulation of Generic Constituents and Addition of New Tracking Capabilities

In addition to simulating water temperature and a wide range of water-quality constituents, CE-QUAL-W2 also can simulate conservative and nonconservative tracers and "generic" constituents defined by various zero- and first-order rate equations. A generic constituent is a modeled concentration of a hypothetical tracer that is subjected to the effects of advection and dispersion, mixing with other waters, evaporation, and optional zero- or first-order reactions whose rates can vary with temperature. (Rates of zero-order reactions do not depend on the concentration of the constituent being modeled, whereas rates of first-order reactions are dependent on the concentration of the constituent being modeled.) The theory and governing equations are well documented in the user manual (Wells, 2019). In this study, CE-QUAL-W2 was used to track the downstream movement of water and heat from various sources, as well as the age of that water and heat, by tagging each input or source with one or more generic constituents. Simple generic tracers have been available in CE-QUAL-W2 for many years, but code changes were required to allow the model to track water, heat, and the ages of water and heat from specific sources.

Code Changes to Track Water Sources

Tracking an individual source of water is relatively straightforward and can be accomplished by defining a generic constituent as the fraction of water from a particular source. Water from the source of interest is tagged with a generic-constituent concentration of 1.0 (in other words, 100 percent) when that water is added to the model, and all other sources of water are tagged with a concentration of zero. The "mass" of the tracer is preserved by setting its zero- and first-order reaction rates to zero, thus making it nonreactive, or "conservative." The generic constituent is then advected, dispersed, and mixed with other sources of water in all the ways that would be expected of a nonreactive tracer. Unlike a dissolved tracer that would tend to increase its concentration when subjected to evaporation, however, a generic constituent tracking water must be allowed to leave the model domain along with any water lost via evaporation. This process is defined according to the following equation:

$$\frac{\partial C_g}{\partial t} = -EA\,C_g/V \qquad (2)$$

where

C_g is the concentration of the generic constituent,
t is time in seconds,
E is the evaporation rate in cubic meters per square meter per second,
A is the surface area through which evaporation occurs, in square meters, and
V is the volume of water remaining, in cubic meters.

A small code change was required to ensure that this evaporative loss occurred. A new user input (CGTYPE) was added to the CE-QUAL-W2 control file to identify this type of generic constituent in a way that the model would recognize and appropriately act upon when accounting for mass lost due to evaporation. See appendix 1 for the details of changes to the generic-constituent inputs in the CE-QUAL-W2 control file, and appendix 2 for a description of changes made to the model source code.

By using these generic tracers in the model, the amount of water released from various upstream dams could be tracked, either separately or together, such that the fraction of water from these sources could be modeled and known at all locations in the model domain. Flow releases from BCL, BLU, CGR, COT, DEX, DOR, FAL, and FOS dams were individually tracked. Releases from Fern Ridge Dam on the Long Tom River were not tracked because the Long Tom River was modeled only as a tributary input in this study. Likewise, releases from several WVP dams (for example, Detroit Dam upstream of Big Cliff Dam [BCL]) did not enter into these computations because of their location upstream of other WVP dams (fig. 1). The fraction of streamflow from all non-dam sources, such as tributaries and point sources, groundwater inputs, and rainfall, was not explicitly tracked by the model but could be calculated as 1.0 minus the sum of the fractional flows from the tracked dam releases.

Code Changes to Track Heat Sources

The heat content of a river is continually affected by incoming and outgoing energy fluxes, with some heat that originated from upstream sources removed by outgoing energy fluxes such as back radiation and evaporation, and replaced with heat from other water sources or incoming EEFs such as short-wave solar radiation and long-wave atmospheric radiation. In this study, several categories of heat sources were tracked by the models: (1) heat from individual upstream dam releases; (2) heat from other sources of water such as tributaries, groundwater, and point sources; and (3) heat from EEFs. Tracking the contribution of each source category to the overall heat content of the stream is similar to tagging the heat from each source category with a different color, as in figure 3. In that way, processes that add heat to the stream would add heat tagged with a single color, whereas processes that remove heat from the stream would remove heat from a mixture of sources. The fraction of heat from each source category being removed would depend on the fraction of each heat source that is present in the stream.

Any heat added to a waterbody, regardless of the source, may be removed from the waterbody at some later time through withdrawals or other water exports, or through any of the processes that export heat across the air/water or sediment/water interfaces, such as evaporation, back radiation, and conduction. These heat-loss processes diminish the percentage of heat in the river from upstream sources as the water moves downstream. Tracking heat from an upstream source is important when trying to determine how far downstream that particular source may have an influence on water temperature. This sort of heat tracking can be accomplished through a modification of the algorithms associated with generic constituents in CE-QUAL-W2. First, however, it is important to define how heat content is quantified.

Heat content typically is defined relative to a reference temperature. Theoretically, the heat content of a water parcel could be defined relative to a reference temperature of absolute zero (0 K, or -273.15 °C), but such a reference would require an accounting of the heat content of ice up to its freezing point, the heat needed to change solid ice to liquid water, and then the heat required to warm liquid water from its freezing point to its actual temperature. A reference state of liquid water at 0 °C is more convenient and straightforward (as long as ice does not form, or negative heat contents are allowed). The computations for this study were focused on conditions occurring from spring through early autumn when ice formation was unlikely; therefore, these computations do not account for the presence, formation, or melting of ice. Using a reference of liquid water at 0 °C, heat content can be defined as:

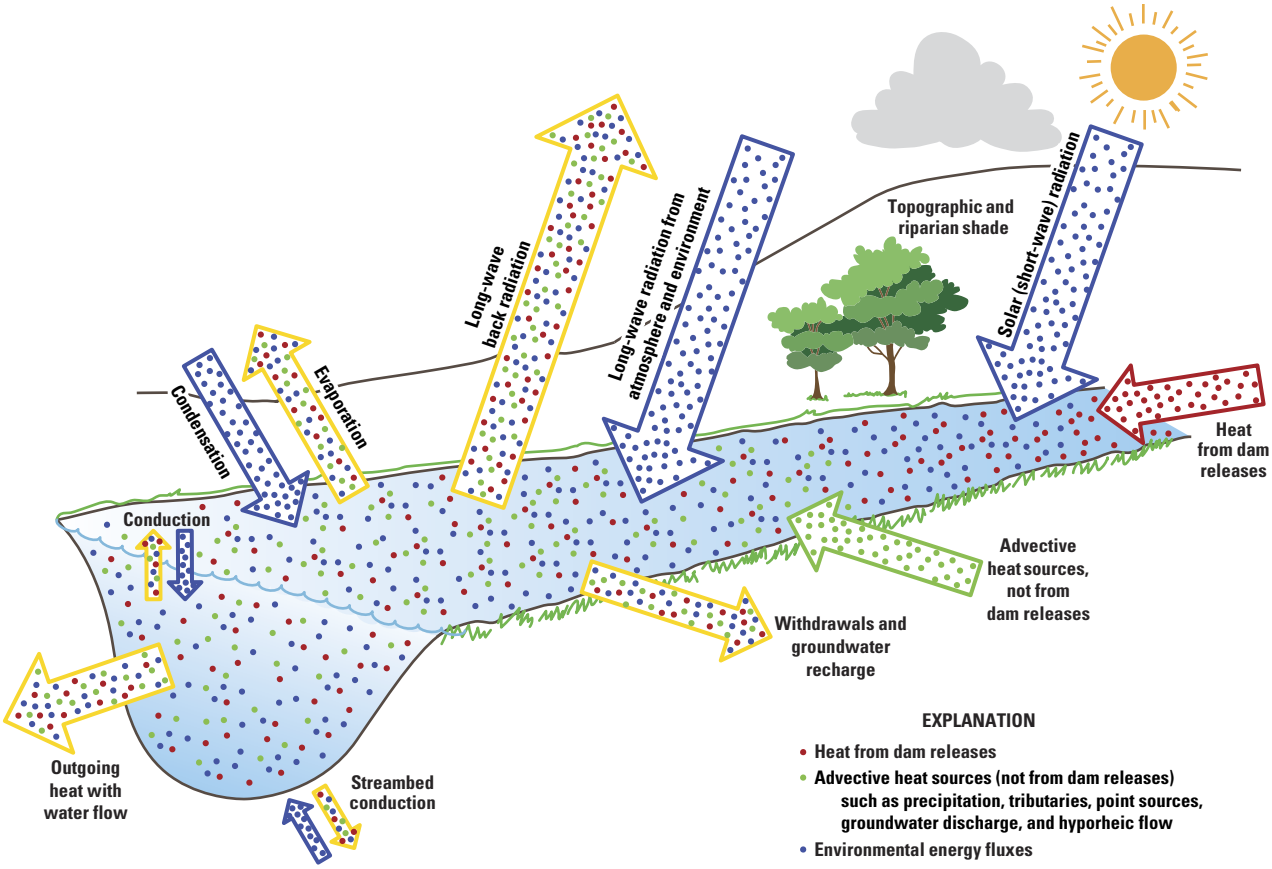

Figure 3. Heat sources to a stream reach, showing how heat from different sources mixes in the stream and how outgoing energy fluxes export heat from a mixture of sources. The colored dots represent heat from different categories of sources. Figure adapted from Bartholow (2000).

$$H = m C_p(T_w - T_{ref}) = \rho V C_p(T_w - T_{ref}) = \rho V C_p T_w \quad (3)$$

where

H is heat content in Joules,
m is the mass of liquid water in kilograms,
C_p is the specific heat of water (4,186 Joules per kilogram per degree Celsius),
T_w is the water temperature in degrees Celsius,
T_{ref} is the reference temperature (0.0 degrees Celsius),
ρ is the density of water in kilograms per cubic meter (about 1,000), and
V is the volume of water in cubic meters.

If water density is assumed to be constant, then heat content relative to liquid water at a reference temperature of 0 °C is a linear function of water temperature. The CE-QUAL-W2 model applies this assumption, allowing the model to essentially transport temperature rather than heat content. This simplification may be thought of as the removal of the constant factor ρC_p from the computations of transport and mixing, and such factors could be added back at any time to convert temperature to heat content.

In the same manner that individual water sources can be tracked, individual sources of heat in CE-QUAL-W2 can be tracked through the use of generic constituents and a few changes in the model source code. Heat entering the model domain with a source of water is easily accounted for by assigning the temperature of that water to the concentration of the generic constituent assigned to track that source of heat. Tracking heat from an upstream dam release, for example, would require the assignment of the temperature of that dam release to the concentration of the generic constituent used to track heat from that upstream dam release. All other sources of water entering the model domain would be assigned a concentration of zero (no heat from the tracked dam release) for that generic constituent. The model simulates advection, dispersion, and mixing with other water sources as it does for all generic constituents. The fraction of heat content from that upstream dam release at any point downstream then would be computed by dividing the concentration of that generic constituent by the temperature of the water at the downstream location.

Code modifications were needed to ensure that the appropriate amount of the heat-related generic constituent is lost with (1) the mass of water lost through evaporation and (2) the heat-loss processes of back radiation, conduction, and evaporation. The loss of water associated with evaporation takes some of the generic constituent with it, and the loss rate is the same as that expressed in equation 2, generally as:

$$\frac{\partial C_s}{\partial t} = -EA\,C_s/V \tag{4}$$

where C_s is the heat (concentration) in the generic constituent from the identified source, and the other variables are defined as they were in equation 2. Equation 4 accounts for the loss of any heat from the identified source that is contained in the water being lost through evaporation.

The process of evaporation, however, also involves a substantial loss of heat from the waterbody due to the phase change of the evaporated water from liquid to vapor. That evaporative heat loss, along with any heat lost due to blackbody back radiation from the water surface and any conductive heat loss across the air/water or sediment/water interfaces, can be expressed as:

$$\frac{\partial C_s}{\partial t} = -H_L(C_s/T_w)A/\rho V C_p \tag{5}$$

where

C_s is the "concentration" of heat tracked from an identified source in degrees Celsius,
t is time in seconds,
H_L is the heat loss rate in Joules per square meter per second,
T_w is the water temperature in degrees Celsius,
A is the surface area through which the heat loss occurs, in square meters,
ρ is the density of water in kilograms per cubic meter (about 1,000),
V is the volume of water from which the heat is lost, in cubic meters, and
C_p is the specific heat of water (4,186 Joules per kilogram per degree Celsius).

The ratio C_s/T_w is the fraction of heat content due to the identified source, such that the entire numerator in equation 5 represents the heat loss rate for the individual source. The denominator simply takes the heat loss rate in the numerator (J/s) and converts the right-hand side of the equation to units of °C/s.

Heat gains from incoming EEFs can be accounted for in a manner similar to equation 5, using the positive (incoming) energy fluxes from short-wave solar insolation, long-wave atmospheric radiation, and any incoming energy fluxes from conduction or condensation. The incoming energy flux would not be added to a generic constituent assigned to track heat from upstream sources or from any specified water input. Rather, this energy flux would be assigned to a separate generic constituent to represent heat originating with EEFs, regardless of whether those fluxes occur across the air/water interface or the sediment/water interface. Outgoing heat fluxes would include a component of this generic constituent as defined in equation 5, and the full equation describing the effects of both incoming and outgoing heat fluxes is:

$$\frac{\partial C_f}{\partial t} = \left(H_G - H_L\left(C_f / T_w\right)\right)A \Big/ \rho V C_p \tag{6}$$

where

C_f is the "concentration" of heat from environmental energy fluxes in degrees Celsius,
H_G is the heat gain rate in Joules per square meter per second,

and all other variables are defined as they were for equation 5.

In this study, generic constituents were configured to track all sources of heat to the river network. Individual generic constituents were configured to account for the heat from (1) initial conditions, (2) one or more specific sources of water such as dam releases, (3) any other sources of water not specifically assigned to other generic constituents, and (4) EEFs across the air/water and sediment/water interfaces. In this way, all of the sources of heat were tracked. As a quality-assurance check, the sum of their concentrations should equal the water temperature at any location. After dividing by the water temperature to compute the fraction or percentage of heat from each source category, their sum should equal 1.0 (or 100 percent).

Code Changes to Track the Age of Water or Heat from Individual Sources

For many years, users of CE-QUAL-W2 have been able to configure one of the generic constituents in the model to compute and track the average modeled "age of water" (often equivalent to an average residence time in lakes and rivers) throughout the model domain. For this modeled age-of-water constituent, all water entering the model from sources outside the model domain, such as upstream boundaries, tributaries, point and diffuse sources, and precipitation, is assigned an age of zero when that water enters the model domain. During each subsequent time step in the model, the age of any water that remains in the model domain is increased by the current time step. This constituent is not meant to characterize the actual age of water moving through a river or reservoir system, but simply the average modeled age of water within the model domain, which, for example, turns out to be useful for quantifying travel time from individual water sources. As with other generic constituents, this tracer is subjected to the effects of advection and dispersion, mixing with other waters, and evaporation. The characteristics of this age-of-water constituent are as follows:

- Initial conditions and inputs of new water are assigned an age (concentration) of zero;
- When evaporation occurs, an appropriate amount of water age must be removed along with the water, as opposed to a dissolved tracer that would become more concentrated in an evaporating pond of water; and
- The water-age constituent is assigned a zero-order reaction rate of -1.0/day as a means of incrementing the age over time.

As in equation 2, the amount of age lost when water leaves the system through evaporation is defined as:

$$\frac{\partial C_a}{\partial t} = -EA\,C_a/V \tag{7}$$

where

C_a is the "concentration" of water age in days,
t is time in seconds,
E is the evaporation rate in cubic meters per square meter per second,
A is the surface area through which evaporation occurs, in square meters, and
V is the volume of water remaining, in cubic meters.

The zero-order reaction rate for water age that enables the model to increment that age with each time step is described simply as:

$$\frac{\partial C_a}{\partial t} = -k = 1.0 \tag{8}$$

where

C_a is the "concentration" of water age, where age is expressed in days,
t is time in days, and
k is a zero-order reaction rate equal to -1.0/day.

The concept of water age and the approach used by CE-QUAL-W2 to compute water age can be extended to track the age of other simulated quantities in the model, such as individual sources of water, total heat content (temperature), and individual sources of heat. The configuration of a generic constituent to track the age of an individual water source or heat source is similar to that used to simulate water age:

- Initial concentrations and all boundary input concentrations are set to zero,
- A zero-order reaction rate is set to -1.0/day, and
- Water loss due to evaporation must also remove some of the generic constituent, as in equations 2, 4, and 7.

Several code changes were needed to handle the evaporative loss, to tie the age calculation to the target source, and to ensure that the zero-order reaction rate was properly computed.

Generic constituents used to track the age of a specific source of water or heat are configured with "concentrations" equal to the age of that source times the concentration of that source. This approach is required because generic constituents used to track heat sources have units of degrees Celsius, which could be multiplied by $\rho V C_p$ to obtain the heat content from each source, or divided by water temperature to obtain the percentage of heat from each source. Similarly, the concentration of a generic constituent used to track age needs to be divided by the concentration of the constituent being age-tracked to obtain the age of that source. Tracking the average water age (water from any source) has been straightforward because the concentration of water is constant and can be ignored (set to 1.0), such that the water-age "concentration" is simply time, or age. A generic constituent used to track the fraction of water from an identified source, however, has a concentration that varies (0.0 to 1.0, as described in section, "Code Changes to Track Water Sources") and dimensionless units, and a generic constituent used to track heat from an identified source has a varying concentration in units of degrees Celsius. A new generic constituent used to track the age of an identified source of water or heat will have units of time multiplied by the concentration of the tracked constituent.

This intrinsic tie between a generic constituent tracking the age of a water or heat source and the constituent being tracked is embodied also in the zero-order reaction rate equation, which had to be modified but still is similar to that used for average water age (eq. 8):

$$\frac{\partial C_a}{\partial t} = -k\,C_s = C_s \tag{9}$$

where

C_a is the "concentration" of the constituent used to track the age of an identified source of water or heat,
t is time in days,
k is a zero-order reaction rate equal to -1.0/day, and
C_s is the concentration of the source of water or heat being age-tracked.

When tracking the average age of water in the system, the concentration of water is constant and C_s can be set to 1.0, causing equation 9 to revert to equation 8. When tracking the average age of all heat in the system, C_s would be set to the water temperature, and the average age of heat in the water would be obtained as C_a/T_w. When tracking the age of an identified source of water or heat, the age of that source of water or heat would be obtained as C_a/C_s. Indeed, this approach can be used to track the average age of water as well as the age of all of the different sources of water, and the average water age could be

separately computed as the sum of the ages of the individual water sources weighted by the fraction of water from each source. The same check could be made for the average age of heat and the ages of heat from all of the various sources. Code changes to enable these new capabilities are described in appendixes 1 and 2.

Customization of Model Outputs

The source code in CE-QUAL-W2 was modified to add or change several customized output files to provide daily and subdaily model results for every segment in the model domain, and to provide detailed energy fluxes and several calculated time scales and dimensionless numbers for every simulated day and every segment in the model domain. The motivation to create or modify these output files was not just to make it easier to post-process the model output and create useful visualizations, but also to search for and discover some useful time scales and ratios that might provide insights into the sensitivity of river temperatures to flow- and temperature-management strategies in the Willamette River system.

Previous customized versions of CE-QUAL-W2 had output files that provided the daily maximum water temperature in every model segment and for each day of the simulation, using either the surface temperature, a volume-averaged temperature, or a flow-weighted temperature for each segment. These output files included daily mean water-quality concentrations and therefore were useful to examine water age, source-tracking, and heat-tracking constituents across the model domain. These output files were modified in this study to include the daily mean and daily minimum water temperature along with the daily maximum, and better controls were added to allow the user to select among these several output files.

One new output file was added to provide daily energy fluxes and several useful time scales and energy ratios for every segment in the model. This new heat-flux output file includes the daily integrated sum of energy fluxes gained across the air/water interface from short-wave solar radiation, long-wave atmospheric radiation, conduction, and condensation, as well as the sum of energy fluxes lost across the air/water interface through blackbody back radiation, evaporation, and conduction. In the model, heat loss through evaporation is a positive number, and when that computed flux is negative, it serves as an estimate of the heat gained through condensation of water vapor on the river surface. Conductive heat fluxes are either gains or losses, depending on the temperature difference between the air and the water surface. For the purpose of this output file, energy gains and losses across the sediment/water interface were not included; such fluxes are typically much smaller than those across the air/water interface in large rivers such as the Willamette River (Sinokrot and Stefan, 1993), and energy fluxes across the sediment/water interface can be complicated by some user settings in the model (Wells, 2019). The new heat-flux output file is described in appendix 3.

Results of Simulations

Willamette River Heat Budgets

The rate at which heat attributable to upstream dam releases in the Willamette River system diminishes downstream from the dams and is replaced by heat from EEFs and other sources depends on the magnitude of EEFs relative to the river's heat content, as well as the modeled width and depth of the river, weather conditions, and other factors. The radiative energy fluxes of the EEFs—short-wave solar radiation and long-wave atmospheric radiation and back radiation—are known to be large and dominant components of heat budgets in large rivers (Edinger and others, 1968; Brown, 1969). The EEF components of the Willamette River heat budget were quantified with the CE-QUAL-W2 model at a relatively wide location (about 116 m in summer) with little shading along the river near Keizer (fig. 1) to illustrate the magnitude and relative importance of these energy fluxes. The total energy gained or lost through EEFs scales linearly with river width, but the fluxes depend on weather conditions (air temperature, wind speed, dew-point temperature, cloud cover, etc.) and river surface temperature. Individual energy fluxes across the air/water interface were computed with CE-QUAL-W2 for several days in 2015: a warm sunny day in mid-summer (July 1), a cloudy day in mid-summer (July 11), a sunny day in late summer (September 10), and a cloudy day in late summer (September 14). These dates were chosen because the river was strongly warming or cooling (indicating a large net heat flux into or out of the river), as reflected by modeled water temperatures (fig. 4). Results of the simulations showed that long-wave atmospheric radiation was consistently the largest energy influx, and highest in summer when air temperature was warmest (table 1). Solar radiation was the next largest energy influx, with large variations during a long sunny day in July compared to that during a shorter cloudy day in September. Back radiation was the largest outgoing EEF, accounting for more than 70 percent of all outgoing EEF on the example dates. Evaporation also was important to the outgoing energy flux, and when added to the back-radiation flux, the two accounted for 95 percent of the outgoing EEF on the example dates. The EEF components varied over the course of the day, such that net heating occurred only during daytime (fig. 5).

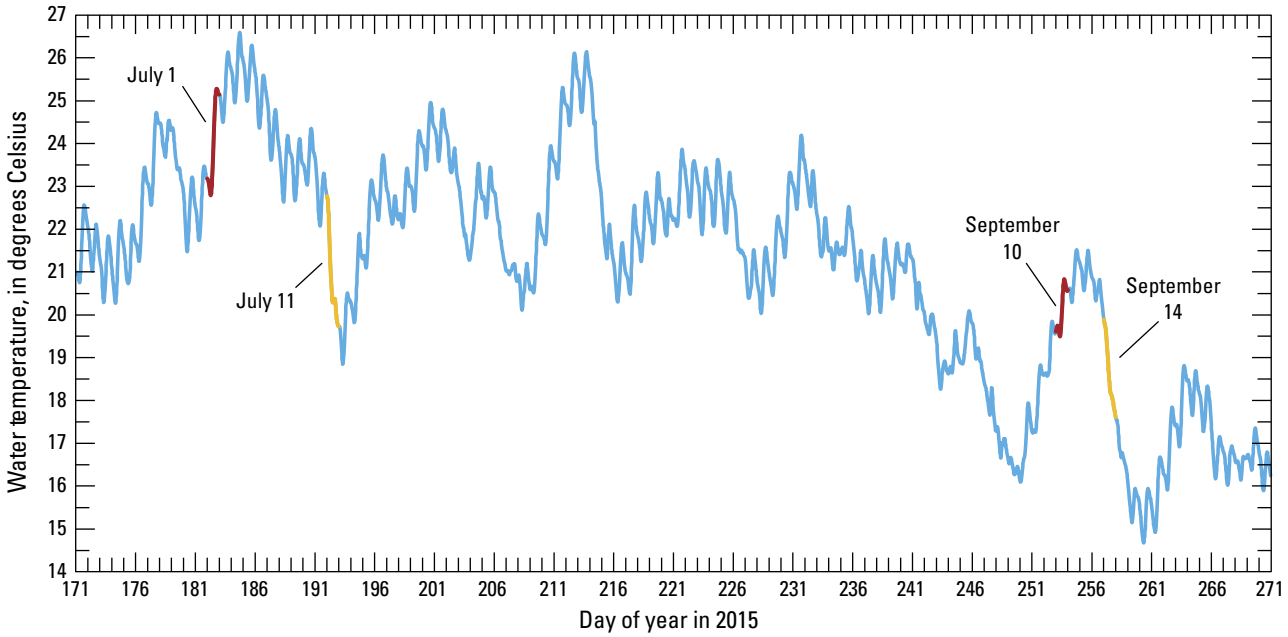

Figure 4. Modeled water temperature in the Willamette River at Keizer, northwestern Oregon, showing four example dates in 2015 when the river was strongly warming or cooling. The modeled river reach at Keizer includes a U.S. Geological Survey temperature measurement station (site 14192015).

Table 1. Individual daily energy fluxes across the air/water interface, as computed by a calibrated CE-QUAL-W2 model over the course of 4 days in the summer of 2015 for a 116-meter wide and 250-meter long reach of the Willamette River near Keizer, Oregon.

[The modeled river reach at Keizer includes a U.S. Geological Survey temperature measurement station (site 14192015). **Abbreviations**: °C, degrees Celsius; gJ, gigaJoules.]

Condition or daily flux	Date and type of day			
	July 1, 2015 sunny mid-summer day	July 11, 2015 cloudy mid-summer day	Sept 10, 2015 sunny late-summer day	Sept 14, 2015 cloudy late-summer day
Daily mean air temperature (°C)	26.5	19.1	21.5	13.9
Daily mean water temperature (°C)	24.0	20.8	20.1	18.6
Incoming Daily Environmental Energy Fluxes				
Long-wave atmospheric radiation (gJ)	946.1	918.0	854.1	733.7
Short-wave solar radiation (gJ)	772.0	228.6	484.0	139.4
Conduction (air/water, gJ)	72.2	6.5	46.2	0.0
Condensation (gJ)	0.0	0.0	0.0	0.0
Subtotal: Incoming fluxes (gJ)	1790.3	1153.0	1384.4	873.2
Outgoing Daily Environmental Energy Fluxes				
Back radiation (gJ)	1081.9	1036.0	1026.3	1005.3
Evaporation (gJ)	426.3	271.9	184.8	285.0
Conduction (air/water, gJ)	19.5	28.4	19.5	70.2
Subtotal: Outgoing fluxes (gJ)	1527.7	1336.3	1230.6	1360.5
Net Incoming Environmental Energy Flux				
Total daily energy flux (gJ)	262.6	-183.3	153.7	-487.4

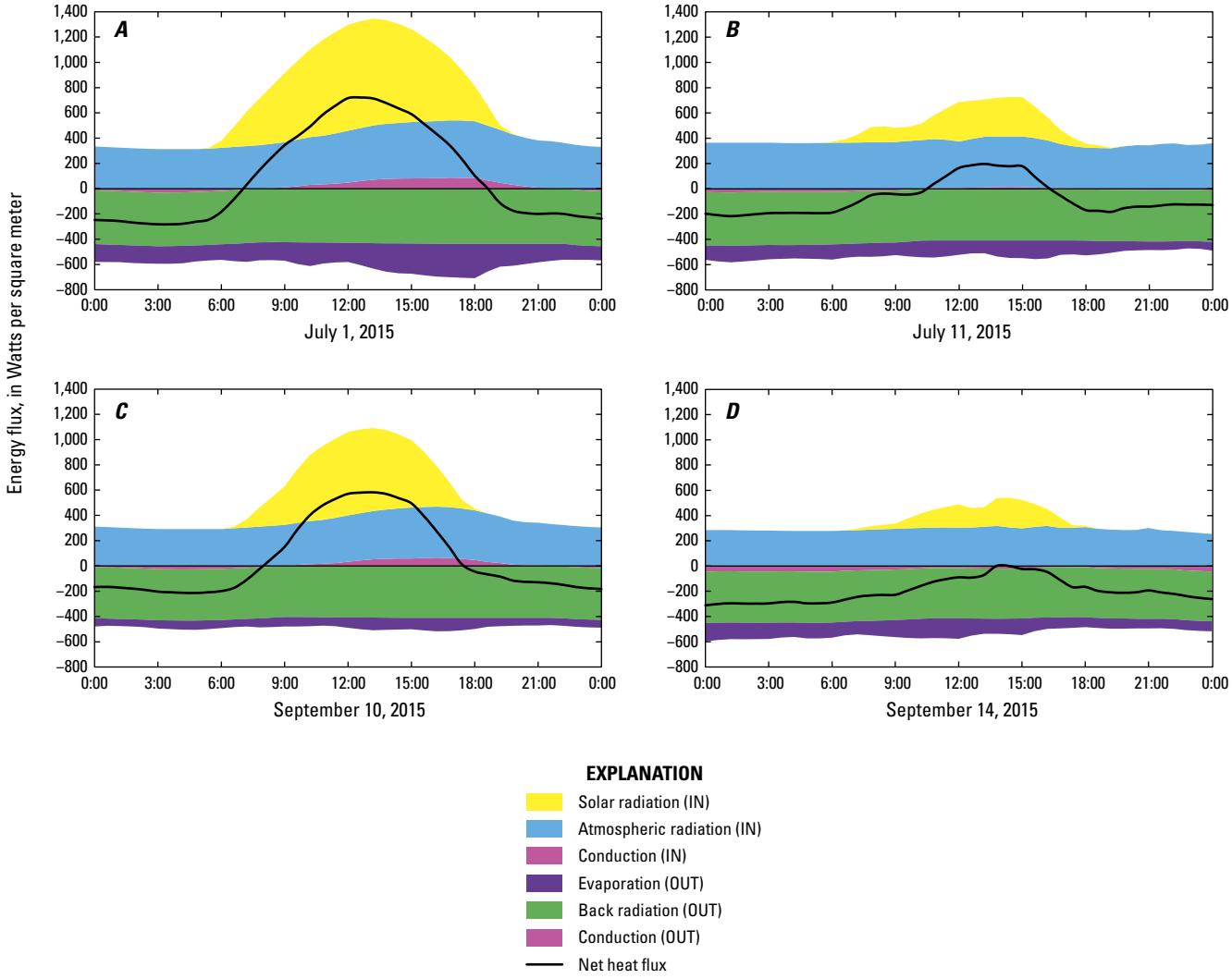

Figure 5. Modeled environmental energy fluxes across the air/water interface of the Willamette River at Keizer, northwestern Oregon, on 4 days in 2015 when the river was strongly warming or cooling: (*A*) a warm sunny day in mid-summer (July 1), (*B*) a cloudy day in mid-summer (July 11), (*C*) a sunny day in late summer (September 10), and (*D*) a cloudy day in late summer (September 14). Fluxes are graphed in a "stacked" manner, such that the graphed regions are additive and no fluxes are hidden behind other fluxes. The modeled river reach at Keizer includes a U.S. Geological Survey temperature measurement station (site 14192015).

The modeled EEFs for the example dates at Keizer (table 1) are substantial relative to the heat content in the river. The daily incoming energy from EEFs for the examples in fig. 5 ranges from 873 to 1,790 gigaJoules (gJ), and the outgoing fluxes account for 1,231 to 1,528 gJ, whereas the heat content for the example 250-meter-long river reach was roughly 3,800 to 4,800 gJ on the example dates in September and 4,300 to 6,500 gJ on the example dates in July. With roughly 1,000 gJ or more of EEFs going into and out of the river each day, and the river holding about 4,000 to 6,000 gJ of heat, weather-related energy fluxes will come to dominate the summertime heat budget and temperature of the river over a relatively short time frame. In these examples, the ratio of the heat content of the river to the total daily incoming EEF ranged from 3.4 to 4.3, suggesting a time scale of roughly 3–4 days over which a substantial amount of the heat content in the Willamette River could be replaced by heat from EEFs. Of course, such heat replacement would take longer if the river were deeper or narrower, and would take less time if the river were wider or shallower. In this example, the width to mean depth ratio was between 71 and 76, but the ratio varies in other reaches of the Willamette River. For example, the river downstream of Newberg is substantially deeper, and some of the more upstream reaches are shallower. Regardless, this examination of the magnitudes and relative importance of the EEF components shows that the largest EEFs are radiative (long wave and short wave) and EEFs are large enough during summer in the Willamette River system to control the river temperature over time scales of several days to a week.

Tracking Sources of Water

Separating streamflow in the Willamette River into components by source allows for a better understanding of the relative importance of releases from individual WVP dams to the streamflow regime in the downstream river. Previous studies have shown that the release of stored water from WVP dams during summer approximately doubles the flow of the Willamette River at Albany and Salem compared to summer baseflow in the pre-dam era (Rounds, 2010). The percentage of summer streamflow in the Willamette River that is traceable to WVP dam releases is consistent with this finding. During the typically dry summer month of August in 2011, 2015, and 2016, the percentage of streamflow that was tracked by CE-QUAL-W2 to upstream dam releases ranged from 53 to 58 percent at Harrisburg, 50 to 54 percent at Albany, and 55 to 59 percent at Salem (monthly means, table 2). An analysis of pre-dam conditions was not part of this study, but these percentages illustrate the dominance of WVP dam releases among the sources of downstream flows during August, which in turn indicates that flow management has the potential to be a useful strategy for altering downstream flow and thermal conditions at that time of year.

Table 2. Percentage of total streamflow in 2011, 2015, and 2016 that was tracked from Willamette Valley Project dam releases to key locations along the Willamette River, northwestern Oregon.

[Results do not include any releases from Fern Ridge Dam on the Long Tom River.]

Willamette River Site	USGS Station Number	Monthly mean streamflow contribution attributable to upstream dam releases (percent)						
		April	May	June	July	August	September	October
				2011				
Owosso Bridge	14158100	63.1	77.8	85.1	85.9	85.8	89.2	89.0
Harrisburg	14166000	39.2	49.1	53.4	50.0	52.7	65.0	65.1
Albany	14174000	32.4	43.5	48.4	45.7	50.4	62.0	54.8
Salem	14191000	37.0	47.8	53.0	48.4	54.7	68.0	64.8
Newberg	14197900	32.4	43.5	51.2	47.2	53.4	66.3	63.1
Willamette Falls	14207740	26.9	37.0	46.2	43.9	49.8	62.7	60.8
				2015				
Owosso Bridge	14158100	54.1	67.8	75.7	79.8	83.8	83.3	83.0
Harrisburg	14166000	25.2	36.4	45.9	52.0	56.7	55.6	57.5
Albany	14174000	19.6	28.9	38.5	46.9	50.2	49.2	47.2
Salem	14191000	21.4	33.1	43.6	51.3	55.6	56.7	54.8
Newberg	14197900	19.1	30.9	41.8	50.0	54.5	55.2	53.6
Willamette Falls	14207740	15.5	26.4	37.5	46.6	51.1	52.0	52.5
				2016				
Owosso Bridge	14158100	60.7	75.1	82.7	81.9	84.0	82.2	67.3
Harrisburg	14166000	34.1	50.8	56.4	52.9	57.5	55.4	43.5
Albany	14174000	27.7	43.7	47.0	47.1	54.0	51.0	32.6
Salem	14191000	32.8	46.7	52.3	53.3	58.7	60.8	40.2
Newberg	14197900	29.9	43.6	50.4	51.0	57.2	57.8	36.7
Willamette Falls	14207740	25.6	38.8	46.4	46.7	54.1	54.4	33.5

The WVP dams that account for the largest fractions of downstream flow generally are the ones that impound the largest upstream reservoirs. The largest reservoirs in the WVP, ranked by full-pool volumes listed by Rounds (2010) from USACE sources, are Lookout Point Lake (455,800 acre-ft, upstream of Dexter Lake), Detroit Lake (455,100 acre-ft, upstream of Big Cliff Lake), Green Peter Lake (428,100 acre-ft, upstream of Foster Lake), Hills Creek Lake (355,500 acre-ft, upstream of Lookout Point Lake), and Cougar Reservoir (219,000 acre-ft). The downstream flow fractions in figure 6 show that releases from these large lakes or from the dams farther downstream of these lakes account for most of the flow from upstream dams in the Willamette River. The percentage of flow sourced from WVP dams varies seasonally; graphs of the streamflow contributions from upstream dam releases show that the fraction of flow from dam releases is relatively large in late summer, but smaller during spring and autumn (fig. 6). In spring, high flows in unregulated streams from runoff of rainfall and snowmelt, combined with smaller dam releases as the WVP reservoirs are filled prior to summer, decrease the relative percentage of streamflow traceable to WVP dams. Conversely, the percentage of flow attributable to individual reservoir releases sometimes rises in September because input from unregulated streams remains low and dam operators need to release stored water and decrease reservoir levels to make room for temporary storage of runoff from autumn storms; such autumn releases did not occur in 2015 to any appreciable extent because 2015 was a dry year, the reservoirs did not fill in spring, and reservoir levels were already sufficiently low in September.

The relative importance of individual dam releases and the seasonal pattern of flow augmentation in the Willamette River is perhaps better illustrated by visualizing the total fraction of streamflow from upstream WVP dam releases over time throughout the model domain. For example, the total fraction of streamflow from the eight tracked upstream dam releases from late March through the end of October of 2015 is shown in figure 7 for the river reach starting at Dexter Dam on the Middle Fork Willamette River and continuing downstream to the Willamette River at Willamette Falls. Most of the flow in the Middle Fork Willamette River and the Willamette River upstream of its confluence with the McKenzie River is traceable to upstream WVP dams, which include Dexter, Fall Creek, Dorena, and Cottage Grove Dams. At the confluence of the McKenzie River, the percentage of flow traced to WVP dams decreases considerably. Although the McKenzie River has two WVP dams on important tributaries (Blue River Dam on Blue River, and Cougar Dam on the South Fork McKenzie River) and several small dams owned by the Eugene Water & Electric Board along the upper McKenzie River, these dams contribute a relatively small amount of the total flow in the McKenzie River, as a large fraction of its flow is from non-dam sources in the higher-elevation, volcanic eastern portion of the Cascade Range. The fraction of water from upstream dams increases at the Santiam River confluence (fig. 7) because a large fraction of the flow in the Santiam River during summer is sourced from releases from Detroit/Big Cliff, Green Peter, and Foster Dams. The boundary between the light-blue and light-orange colors in figure 7 represents the dates and locations where half of the 2015 streamflow was attributable to releases from upstream WVP dams, demonstrating that during late summer, at least half of the flow at most locations in the Willamette River was sourced from upstream dam releases, but that unregulated streamflow contributes more water to the Willamette River during spring. In relatively wet years like 2011, when all of the WVP reservoirs filled in spring, the percentage of flow traceable to WVP dam releases was somewhat greater during April-October due to the availability of more stored water (table 2). In all three of the modeled years, at least half of the late-summer flow was often attributable to upstream dam releases, even in 2015, a dry year in which the WVP reservoirs fell well short of filling in spring, and in 2016, a less-extreme hydrologic year than 2015 in which some of the reservoirs did not fill.

Tracking Sources of Heat

Model simulations in this study showed that EEFs move a substantial amount of heat across the air/water interface each day relative to the heat content of the modeled stream. As time elapses and water moves downstream, therefore, the fraction of heat from an upstream source will gradually be replaced by heat from the surrounding environment. The rate of replacement depends on river width and depth, river temperature, and weather conditions, but the downstream trend will be one of increasing replacement of heat from upstream sources with heat from EEFs and other sources.

Results of the simulations show some interesting patterns in temperature and heat sources with downstream distance in the Willamette River. First, and as expected during the warm and typically dry summers of western Oregon, river temperature tends to increase with downstream distance. Mean water temperatures in August increased about 3.1 °C from Owosso Bridge (19.6 °C) in Eugene to Willamette Falls (22.7 °C) in the hot and dry summer of 2015, about 3.2 °C (19.1 to 22.3 °C) over the same distance in the warm but less-extreme summer of 2016, and as much as 5.7 °C (15.2 to 20.9 °C) over that distance during the cool and higher-flow conditions of 2011 (table 3). River temperatures reflected the cooler weather conditions during 2011, whereas warm weather and low streamflow caused the river to warm rapidly during June of 2015. Second, despite the fact that roughly half of the water in the Willamette River downstream of the McKenzie River may be tracked to upstream dam releases during late summer, the amount of heat in the river that could be tracked to upstream dam releases during August of 2011, 2015, and 2016 diminished from a range of 57 to 59 percent at Owosso Bridge and 26 to 32 percent at Harrisburg to only 12 to 13 percent at Keizer and about 9 percent at Newberg (table 4; fig. 8).

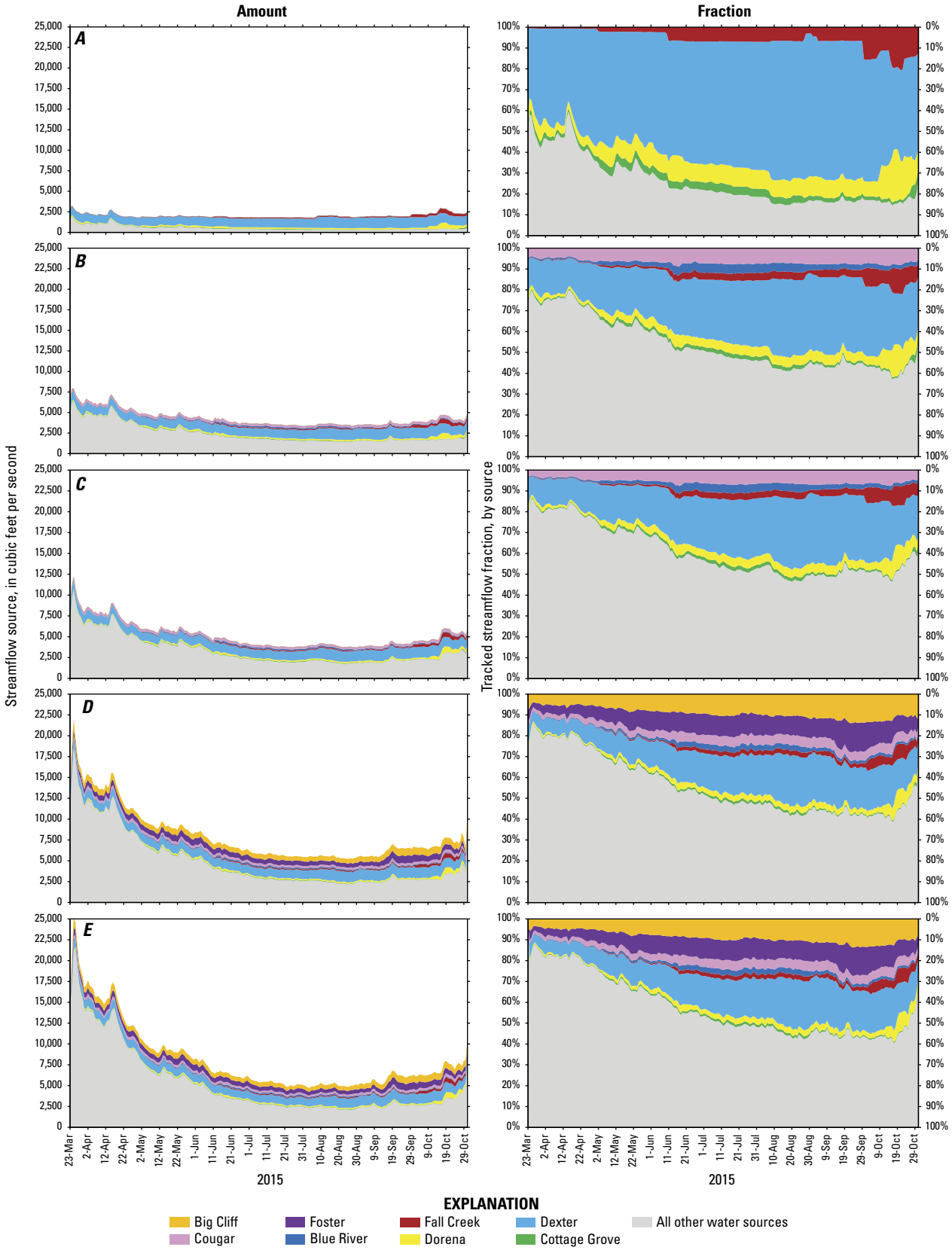

Figure 6. Amount (left column) and fraction (right column) of streamflow in 2015 attributable to upstream dam releases in the Willamette River, northwestern Oregon, at (*A*) Owosso Bridge in Eugene, (*B*) Harrisburg, (*C*) Albany, (*D*) Salem, and (*E*) Newberg. Contributions to streamflow are graphed in a "stacked" manner, such that the graphed regions are additive and no flow contributions are hidden behind others.

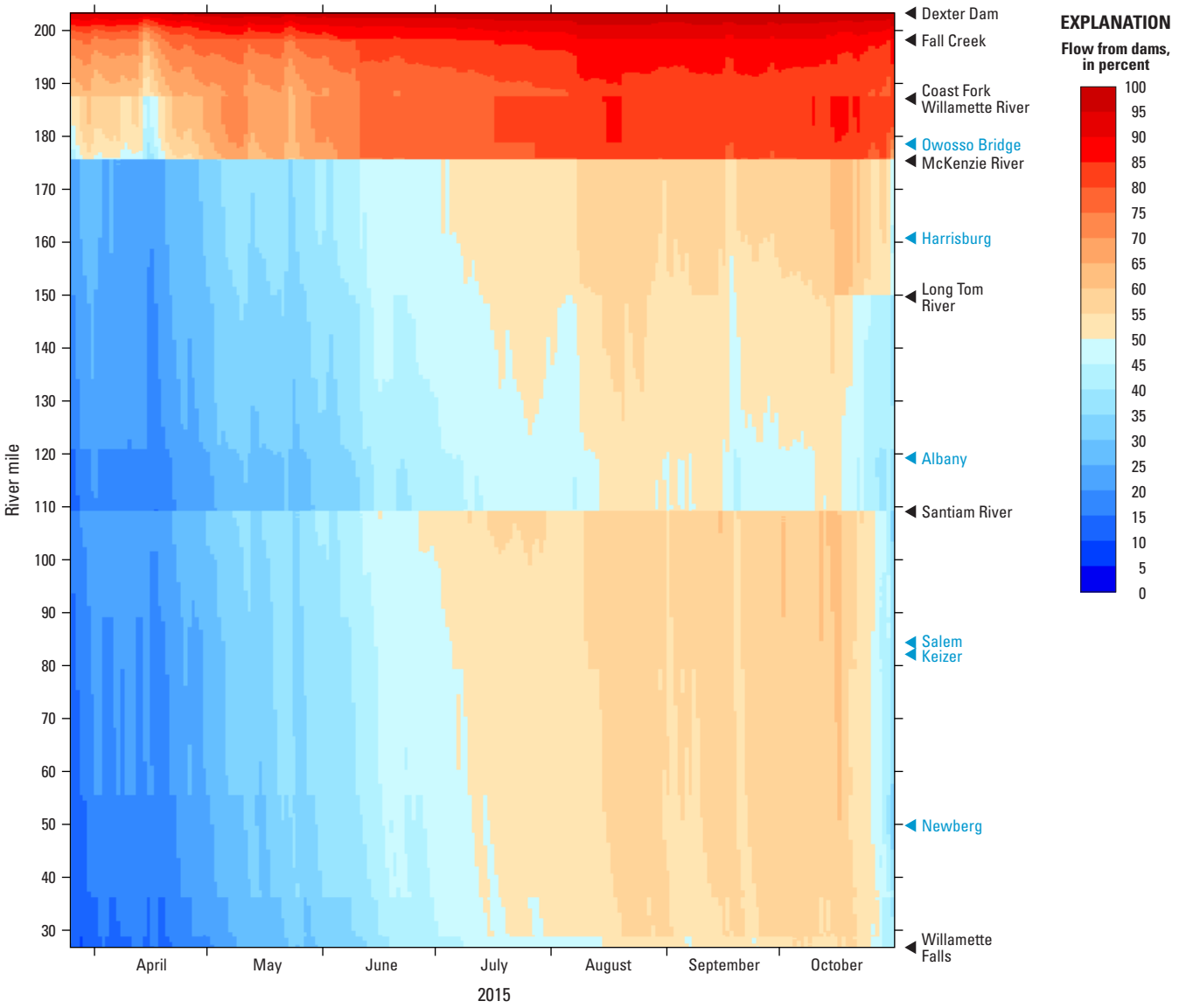

Figure 7. Daily mean fraction of streamflow attributable to eight tracked upstream dam releases for the river reach starting in the Middle Fork Willamette River at Dexter Dam and continuing downstream in the Willamette River to Willamette Falls, northwestern Oregon, late March–October 2015.

These results demonstrate that sufficient time elapses as water moves from upstream dam locations to downstream river locations for most of the heat content in water released from upstream dams to be replaced by heat from other sources and the surrounding environment. The percentage of river heat content derived from EEFs during August of 2011, 2015, and 2016 ranged from 30 to 32 percent at Owosso Bridge to 52 to 54 percent at Harrisburg, 69 to 73 percent at Keizer, and 75 to 79 percent at Newberg (table 5; fig. 8). The percentages of heat content attributable to upstream dam releases at these downstream locations sometimes increased in late summer and autumn, for two reasons: (1) some WVP dams release unseasonably warm water in late summer and autumn and warmer water has more heat relative to a reference condition of liquid water at 0 °C and (2) the river does not tend to warm as much in autumn as it does in mid-summer because of a smaller net influx of heat from EEFs and other sources. Releases in September or October occur as reservoir levels are being drawn down in preparation for the storage of runoff from autumn and winter storms, and that drawdown tends to bring warmer surface water in the reservoirs (water that was warmed in mid-summer) closer to the elevation of the outlet structures (Rounds, 2007; Rounds, 2010; Buccola and others, 2016; Buccola, 2017).

Table 3. Monthly mean modeled water temperatures in 2011, 2015, and 2016 at key locations along the Willamette River, northwestern Oregon.

Willamette River Site	USGS Station Number	Monthly mean water temperature (degrees Celsius)						
		April	May	June	July	August	September	October
				2011				
Owosso Bridge	14158100	8.1	9.6	12.2	15.0	15.2	14.9	14.5
Harrisburg	14166000	8.6	10.3	13.1	16.2	16.8	14.9	12.9
Albany	14174000	9.2	11.1	14.2	17.8	18.5	15.9	13.4
Keizer	14192015	9.0	11.0	14.1	18.4	19.5	16.2	12.6
Newberg	14197900	9.4	11.5	14.6	18.8	20.3	16.8	12.7
Willamette Falls	14207740	9.6	11.8	14.9	19.0	20.9	17.5	12.8
				2015				
Owosso Bridge	14158100	11.5	13.9	17.5	19.7	19.6	17.8	15.6
Harrisburg	14166000	11.5	14.6	18.6	20.4	19.7	16.8	14.2
Albany	14174000	12.2	15.8	20.4	22.4	21.4	17.7	14.7
Keizer	14192015	12.2	16.1	21.1	23.1	21.9	17.7	14.7
Newberg	14197900	12.5	16.4	21.5	23.3	22.2	17.8	14.7
Willamette Falls	14207740	12.6	16.4	21.6	23.8	22.7	18.3	14.8
				2016				
Owosso Bridge	14158100	10.5	11.9	15.0	17.8	19.1	17.7	14.2
Harrisburg	14166000	11.4	13.0	16.3	18.6	18.9	16.5	12.7
Albany	14174000	12.3	14.3	18.1	20.7	21.0	17.7	13.5
Keizer	14192015	12.5	14.7	18.7	21.2	21.4	17.1	12.9
Newberg	14197900	13.0	15.2	19.0	21.3	21.8	17.2	13.1
Willamette Falls	14207740	13.4	15.5	19.1	21.4	22.3	17.6	13.4

Table 4. Percentage of total heat content in 2011, 2015, and 2016 that is attributable to Willamette Valley Project dam releases at key locations along the Willamette River, northwestern Oregon.

[Results do not include any releases from Fern Ridge Dam on the Long Tom River.]

Willamette River Site	USGS Station Number	Monthly mean heat content attributable to upstream dam releases (percent)						
		April	May	June	July	August	September	October
				2011				
Owosso Bridge	14158100	45.3	59.2	65.4	58.5	57.1	67.2	72.5
Harrisburg	14166000	20.9	26.8	29.4	24.6	25.5	39.6	46.7
Albany	14174000	13.9	18.9	21.2	16.6	17.4	28.1	30.9
Keizer	14192015	12.9	18.1	20.3	13.1	13.0	22.5	28.9
Newberg	14197900	9.5	13.5	16.5	10.3	9.4	16.9	22.8
Willamette Falls	14207740	7.1	10.1	13.3	8.4	6.9	13.0	18.7
				2015				
Owosso Bridge	14158100	33.2	41.3	46.2	51.0	57.4	59.8	61.4
Harrisburg	14166000	11.6	16.1	20.5	24.6	30.5	32.7	36.2
Albany	14174000	6.3	8.7	11.6	14.6	18.0	19.6	21.0
Keizer	14192015	5.1	6.8	8.5	9.9	12.4	15.2	16.5
Newberg	14197900	3.5	4.8	6.0	6.8	8.5	10.5	11.8
Willamette Falls	14207740	2.4	3.4	4.2	4.8	5.8	7.2	8.9
				2016				
Owosso Bridge	14158100	42.8	58.2	59.4	57.3	58.6	59.8	50.9
Harrisburg	14166000	17.8	29.3	30.7	28.7	31.9	33.1	27.6
Albany	14174000	11.1	19.1	18.3	17.4	20.1	20.3	15.3
Keizer	14192015	10.5	14.7	14.5	13.0	13.3	16.2	17.9
Newberg	14197900	7.7	11.0	10.9	9.4	9.3	11.3	13.1
Willamette Falls	14207740	5.8	8.4	8.5	7.0	6.8	8.1	10.1

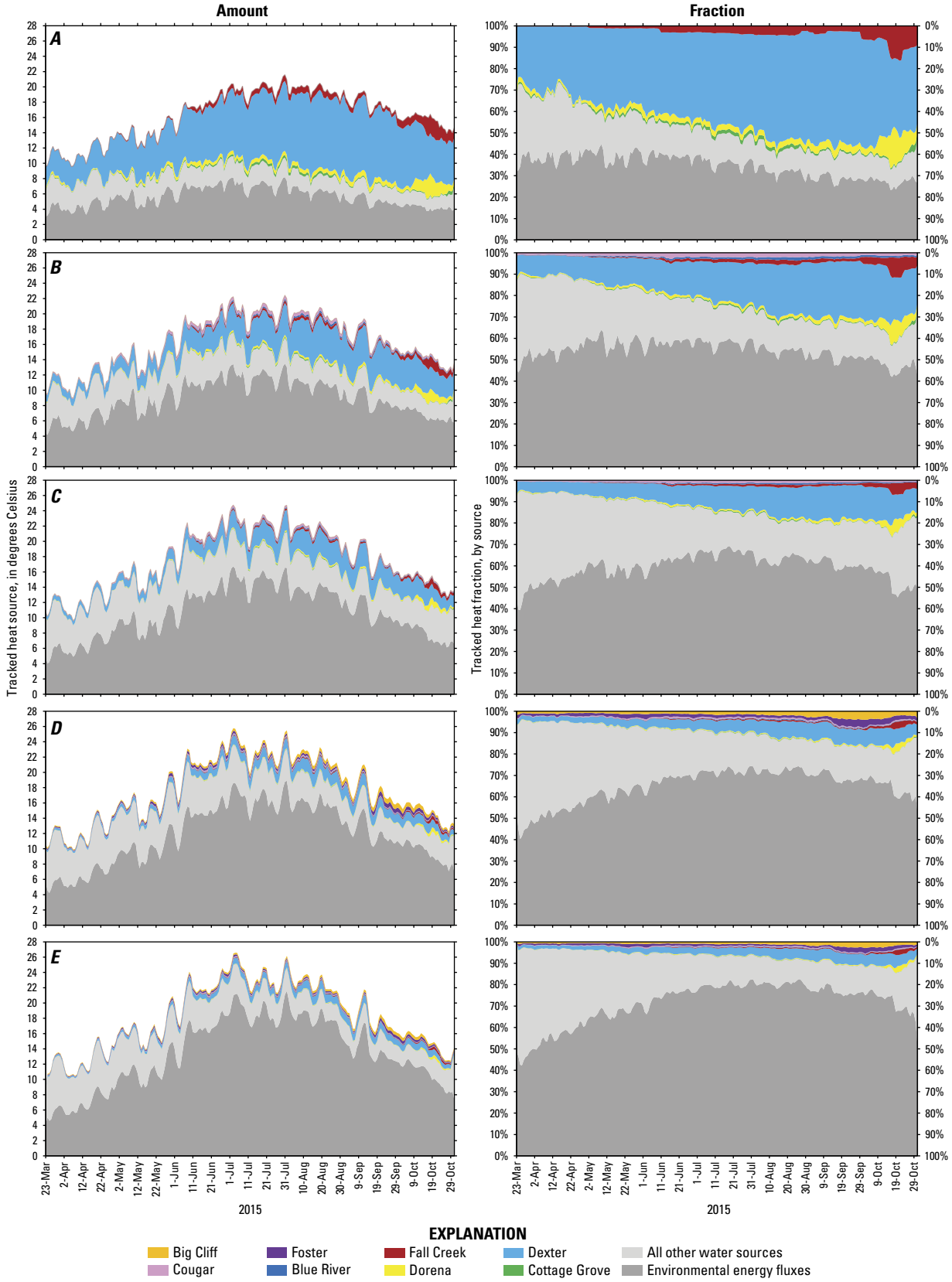

Figure 8. Amount and fraction of heat content attributable to upstream dam releases in the Willamette River, northwestern Oregon, at (*A*) Owosso Bridge in Eugene, (*B*) Harrisburg, (*C*) Albany, (*D*) Keizer, and (*E*) Newberg, 2015. Contributions to heat content are graphed in a "stacked" manner, such that the graphed regions are additive and no heat contributions are hidden behind others.

Table 5. Percentage of total heat content in 2011, 2015, and 2016 that is attributable to environmental energy fluxes (EEFs) at key locations along the Willamette River, northwestern Oregon.

Willamette River Site	USGS Station Number	Monthly mean heat content attributable to environmental energy fluxes (percent)						
		April	May	June	July	August	September	October
2011								
Owosso Bridge	14158100	27.8	24.7	24.2	32.0	31.9	24.7	18.9
Harrisburg	14166000	44.6	47.3	48.3	52.1	51.8	43.4	35.5
Albany	14174000	44.6	49.9	52.3	58.8	62.7	54.9	41.2
Keizer	14192015	48.4	52.2	54.2	62.3	68.9	63.2	50.4
Newberg	14197900	48.1	54.2	58.7	67.9	75.1	70.2	57.7
Willamette Falls	14207740	42.7	49.5	55.9	67.1	75.6	72.5	61.0
2015								
Owosso Bridge	14158100	37.9	38.8	38.2	35.5	31.6	28.4	27.1
Harrisburg	14166000	53.8	58.0	57.6	57.8	54.2	51.4	47.4
Albany	14174000	53.8	58.9	61.9	66.7	63.0	61.0	53.2
Keizer	14192015	53.0	62.0	67.7	71.9	72.2	69.1	64.0
Newberg	14197900	56.1	66.8	73.8	78.3	79.2	76.0	70.8
Willamette Falls	14207740	51.7	64.2	73.5	79.0	80.6	77.8	74.4
2016								
Owosso Bridge	14158100	28.6	22.5	28.8	30.1	30.3	28.2	24.2
Harrisburg	14166000	48.3	44.8	50.5	52.7	52.4	51.5	42.8
Albany	14174000	49.4	50.1	54.5	61.4	64.7	63.0	41.9
Keizer	14192015	52.6	57.5	64.0	69.9	73.0	70.2	43.2
Newberg	14197900	55.3	61.9	69.5	74.6	79.0	74.9	46.7
Willamette Falls	14207740	51.4	59.8	68.3	74.0	79.9	76.5	46.9

The replacement of heat from upstream dams by heat from other water sources and from EEFs is strongly dependent on the elapsed time since release (and thus, distance downstream) from those dams. This dependence becomes evident through an examination of patterns in time/distance color maps of the fraction of heat content in the river from several categories of heat sources (fig. 9). In this example from 2015, it is apparent that heat from dam releases accounts for more than half of the river's heat content only at Willamette River locations upstream of the McKenzie River confluence (orange to red colors in fig. 9*A*; table 4), in the South Fork McKenzie River upstream of the McKenzie River (fig. 9*B*), and locations in relatively close proximity to upstream dams in the North Santiam (fig. 9*C*) and the South Santiam Rivers (fig. 9*D*). EEFs account for more than half of the heat content in the Willamette River at most locations downstream of the McKenzie River during April-October of 2015, with percentages increasing downstream and approaching 80 percent in August at and downstream of Newberg (fig. 9*E*; table 5). The heat content attributable to water sources other than dam releases in the Willamette River during April-October of 2015 was somewhat minor, and as low as 15 percent or so during August at the more downstream locations (fig. 9*F*).

The decrease in the percentage of heat attributable to upstream dam releases as water moves downstream is caused by several processes: dilution from other water sources, warming of the river and the introduction of heat from EEFs, and the export of some dam-sourced heat through outgoing back radiation and evaporation and conduction. The effects of dilution can be at least partially removed by dividing the percentage of dam-sourced heat by the percentage of dam-sourced water; an examination of that ratio illustrates just how quickly the heat from upstream dams is exported from the river or diluted by other sources of heat as the water warms when moving downstream (fig. 10). The percentage of river heat content attributable to upstream dam releases is shown in figure 10*A*, whereas the ratio of the percentage of dam-sourced heat to the percentage of dam-sourced streamflow is shown in figure 10*B*. The latter essentially removes the effect of dilution due to other water sources if those other water sources had the same temperature as the river at their input location. Even accounting for such dilution, the heat attributable to upstream dam releases in 2015 still diminishes to less than 50 percent somewhere between Harrisburg and Albany during late summer and falls to less than 20 percent downstream of Newberg, which is consistent with the increase and predominance

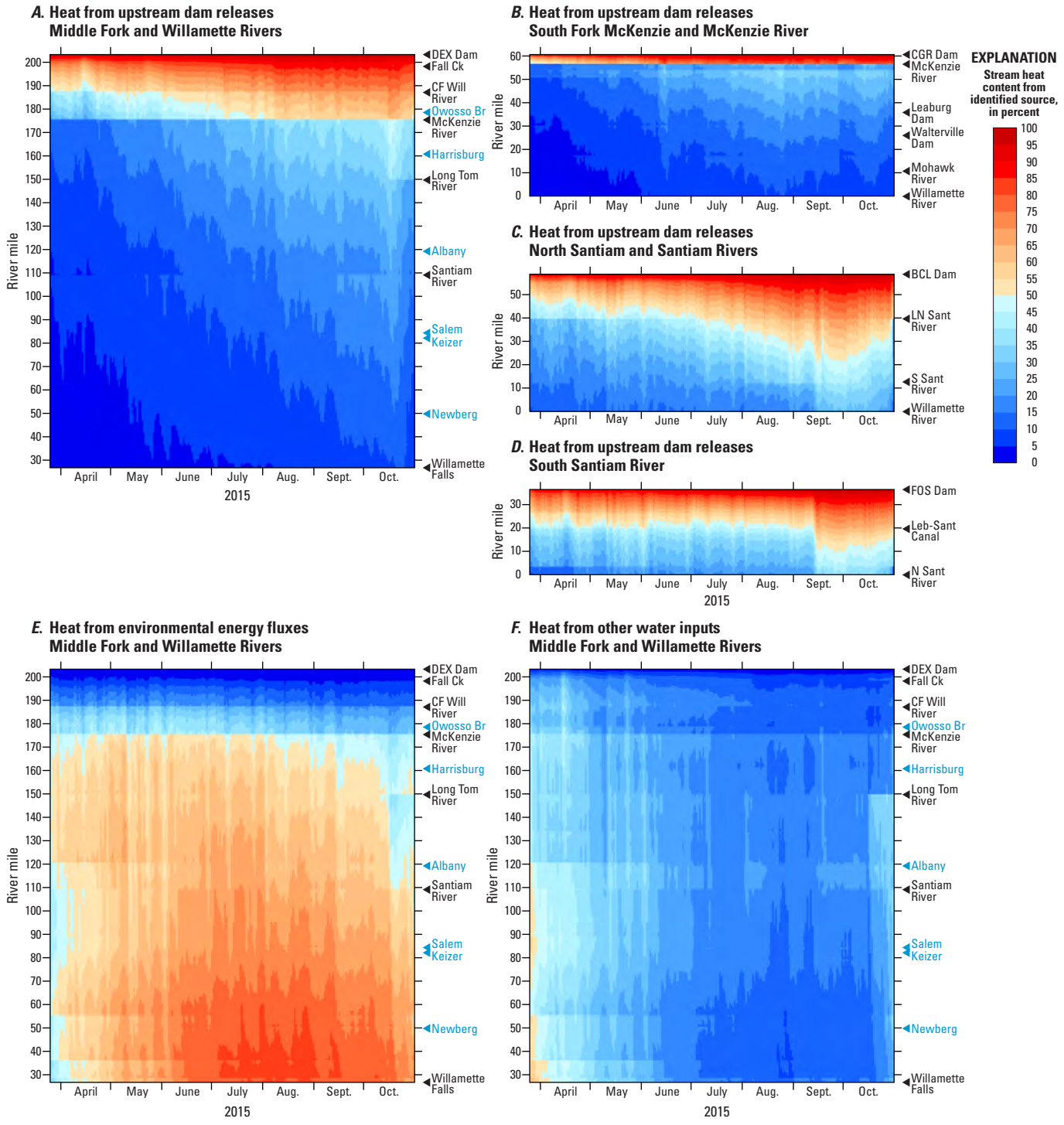

Figure 9. Percentage of stream heat content attributable to (*A*) upstream dam releases in the Middle Fork Willamette and Willamette Rivers, (*B*) upstream dam releases in the South Fork McKenzie and McKenzie Rivers, (*C*) upstream dam releases in the North Santiam and Santiam Rivers, (*D*) upstream dam releases in the South Santiam River, (*E*) environmental energy fluxes in the Middle Fork Willamette and Willamette Rivers, and (*F*) water inputs not associated with dam releases in the Middle Fork Willamette and Willamette Rivers, northwestern Oregon, March–October 2015. Abbreviations: DEX, Dexter Dam; CGR, Cougar Dam; BCL, Big Cliff Dam; FOS, Foster Dam; Ck, Creek; CF, Coast Fork; Br, Bridge; LN, Little North; Sant, Santiam; Will, Willamette. Annotated locations in blue are measurement stations; those in black are tributaries, withdrawals, or model boundaries.

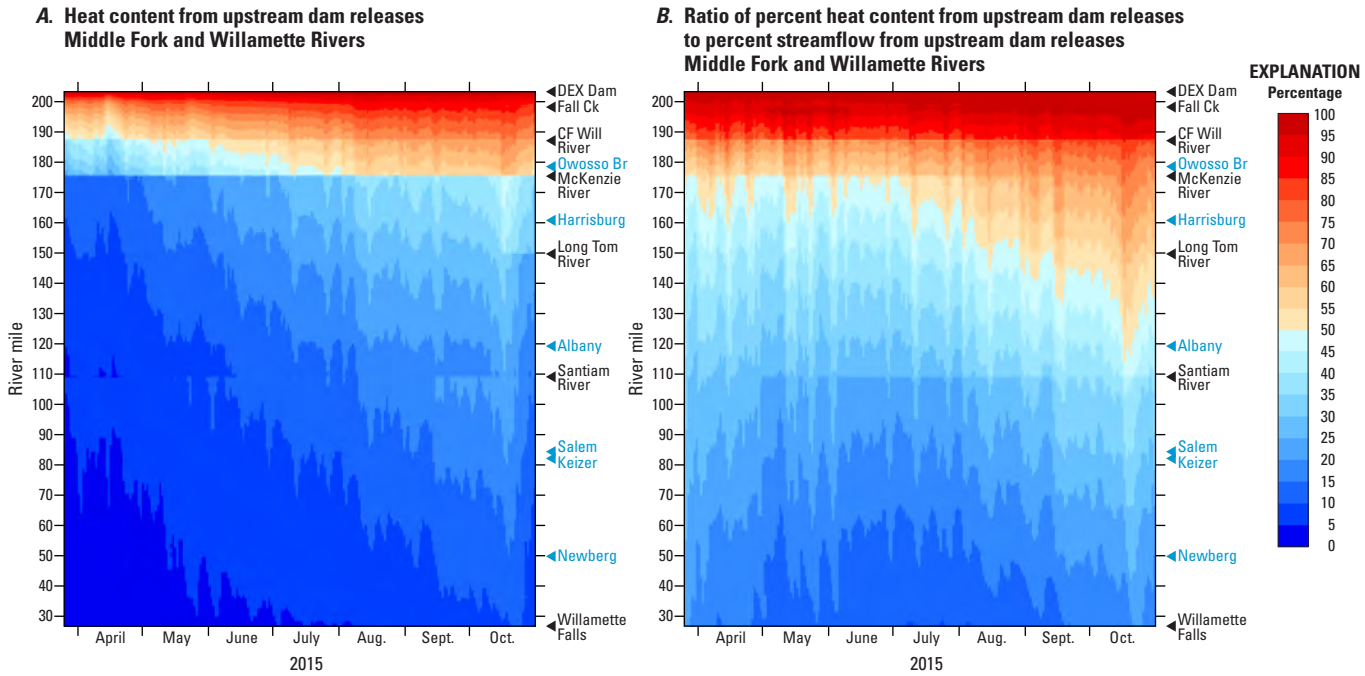

Figure 10. The (*A*) percentage of stream heat content attributable to upstream dam releases and (*B*) percentage of stream heat content attributable to upstream dam releases divided by the percentage of streamflow attributable to upstream dam releases, Middle Fork Willamette and Willamette Rivers, northwestern Oregon, late March–October 2015. Abbreviations: DEX, Dexter Dam; Ck, Creek; CF, Coast Fork; Br, Bridge; Will, Willamette. Annotated locations in blue are measurement stations; those in black are tributaries or model boundaries.

of heat derived from EEFs at those downstream locations. Clearly, the heat content in water from upstream dam releases still is important at sites closer to those dams, such as Owosso Bridge and Harrisburg, but it has less of an influence at more downstream sites.

The increasing replacement of heat from upstream dam releases by heat from EEFs and other water sources with downstream distance in the Willamette River has critical ramifications for the management of water resources and the quantity and quality of habitat for native and anadromous fish species that are sensitive to temperature. The careful management of streamflow throughout the river system downstream of WVP dams has a marked effect on water volume, water level, and transit time. Although water released from dams has an important direct effect on water temperature near the dams, that effect decreases with time and downstream distance. Results from this study indicate that management strategies for water temperature at locations that are several days of travel time downstream of WVP dams would benefit from a recognition that those downstream temperatures (1) have little dependence on dam-release temperatures and (2) are affected by dam releases mainly through decreases in residence time and increases in thermal mass that increase the river's resistance to warming. Earlier research by Rounds (2010) showed that near the largest WVP dams, stream temperature was controlled mainly by the temperature of dam releases and that dam operations could alter the near-dam stream temperature by as much as 6 °C or more relative to a no-dams reference condition. Downstream of the McKenzie River confluence but upstream of the Santiam River confluence, the maximum effect in the Willamette River decreases to less than 3 to 4 °C with a typical magnitude of about 1.5 °C. Downstream of the Santiam River, the maximum effect decreases to less than 2.5 °C and typically less than 1 °C (Rounds, 2010). Results from this study confirm the concepts described by Rounds (2010) by tracking the magnitude of various sources of heat as water moves through the river network, demonstrating that the heat content from upstream dam releases at more-downstream river locations is small and has largely been replaced by heat from EEFs and other sources. In a less scientific sense, one could say that at the more downstream locations, the river has virtually "forgotten" the temperature that the water had when it was released from the upstream dams, consistent with the concept of a "thermal recovery distance" downstream of dams that was discussed and quantified by other researchers (Ward, 1985; Palmer and O'Keefe, 1989; Preece and Jones, 2002). The increasing dependence of downstream locations on heat from the surrounding environment also is consistent with recent findings by Stratton Garvin and others (2022b) that accurate regression models (mean absolute error approaching 0.5 °C) can be constructed to predict water temperature at Willamette River sites based solely on air temperature (as a surrogate for weather conditions) and streamflow (as a surrogate for residence time and heat capacity), showing that the dependence of river temperature on upstream dam-release temperatures diminishes with downstream distance from the dams.

Tracking the Ages of Water and Heat

Using the CE-QUAL-W2 model to track the average ages of water and heat, along with the ages of water and heat from specific sources, provides another method for analyzing the transient nature of heat in river systems. As described earlier in this report, the model has been modified to allow it to track the average age of water or heat, or the age of specific sources of water or heat, by setting the age of new inputs of water or heat to zero and incrementing the age of any water or heat that remains in the system as time elapses in the model simulation. The age of water and heat released from upstream dams continually increases as that water moves downstream, and although some of that water or heat may be lost from the system, such losses do not affect the age of the water or heat from upstream dams that remains in the system. The average age of water or heat in the system is affected by the mix of sources of water and heat to the system, where the average age is equal to the sum of the ages of each source weighted by the fraction of water or heat from each source. The modeled age of water (or heat) from individual upstream dam releases also provides a continuous record of the time required for water to travel from each upstream dam to any downstream location.

A comparison of the average age of water to the average age of heat in the Willamette River system reveals the importance of EEFs in the mix of heat sources. Large EEFs continually move heat into and out of the river across the water surface, bringing "new" heat into the river with an initial age of zero. Ignoring the water-mass effects of condensation, which is an inconsequential process during the dry summer months in western Oregon (table 1), EEFs do not introduce any new water into the river and thus do not affect the average age of water. Consequently, the EEFs cause the average age of heat in the river to be consistently "younger" than the average age of water in the river. In the Willamette River system, the ages of water and heat initially are zero or near zero close to the dams because all of the water and heat in the system close to the dams was sourced from dam releases. As water moves downstream, the average ages of water and heat increase, but the EEFs keep the average age of heat smaller than the average age of the water. For example, the average age of water during August of 2015 at Salem was about 2.7 days, whereas the average age of heat at that time and location was about 1.6 days (figs. 11*A–B*). Farther downstream at Newberg, the ages of water and heat during August of 2015 were about 4.1 and 2.3 days, respectively. At locations downstream of the McKenzie River, the average age of heat was only about 56 to 66 percent of the average age of water in the Willamette River during August of 2015 (figs. 11*C-F*; table 6). These percentages reinforce the concept that heat is a transient quantity, with large fluxes of heat continually moving into and out of the system; therefore, the heat content of the water is always as young as or younger than the water itself. Interestingly, when tracking the age of water and the age of heat from the same individual upstream source, those two ages were found to be identical. Such equivalence makes sense, as the water and heat are tracked from the same source and no other source (or sink) of water or heat can alter the rate at which that water or heat ages as it moves downstream. Although the percentage of heat in the river from an individual upstream source may decrease faster than does the percentage of water from the same source, because the heat in the river has an accelerated loss rate to the environment relative to that of the water, that difference in the percentage does not affect the age of the water or heat from that source that remains in the river.

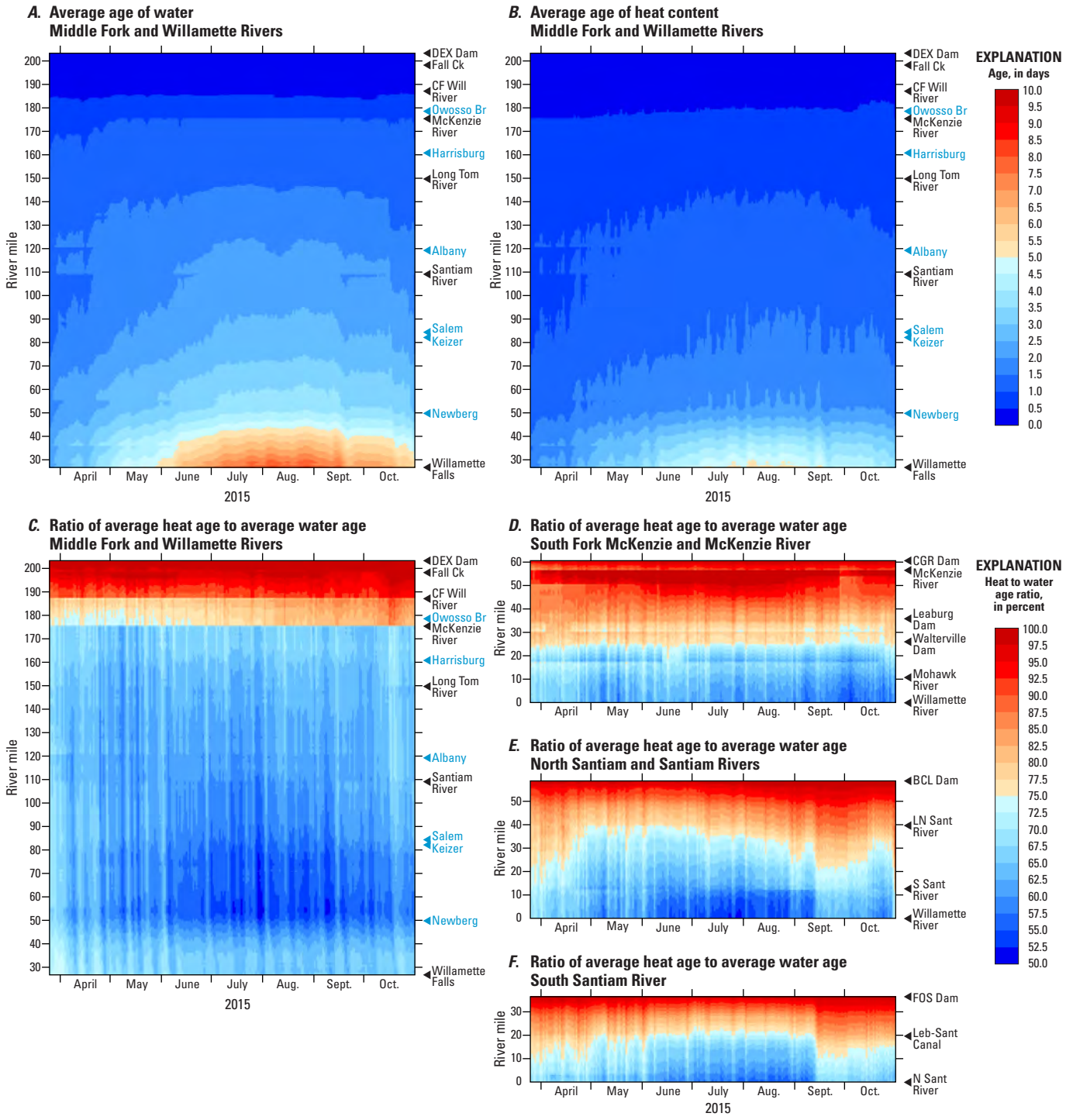

Figure 11. The (*A*) average age of water and (*B*) average age of heat content in the Middle Fork Willamette and Willamette Rivers, as well as the ratio of average heat age to average water age in (*C*) the Middle Fork Willamette and Willamette Rivers, (*D*) the South Fork McKenzie and McKenzie Rivers, (*E*) the North Santiam and Santiam Rivers, and (*F*) the South Santiam River, northwestern Oregon, late March–October 2015. Abbreviations: DEX, Dexter Dam; CGR, Cougar Dam; BCL, Big Cliff Dam; FOS, Foster Dam; Ck, Creek; CF, Coast Fork; Br, Bridge; LN, Little North; Sant, Santiam; Will, Willamette. Annotated locations in blue are measurement stations; those in black are tributaries, withdrawals, or model boundaries.

Table 6. Ratio of the average age of heat to the average age of water in 2011, 2015, and 2016 at key locations along the Willamette River, northwestern Oregon.

Willamette River Site	USGS Station Number	Monthly mean ratio of the average age of heat to the average age of water (percent)						
		April	May	June	July	August	September	October
				2011				
Owosso Bridge	14158100	84.3	85.1	85.6	80.8	80.3	86.5	89.3
Harrisburg	14166000	72.1	69.8	70.1	69.1	68.7	72.3	74.3
Albany	14174000	70.5	68.4	68.5	65.1	64.4	68.1	72.1
Salem	14191000	71.7	70.3	70.1	63.8	60.8	65.0	71.7
Newberg	14197900	69.5	67.6	68.5	62.6	58.9	61.9	68.2
Willamette Falls	14207740	72.5	70.7	71.6	69.3	66.8	68.1	71.9
				2015				
Owosso Bridge	14158100	74.8	75.1	76.2	77.9	80.4	81.9	83.8
Harrisburg	14166000	66.0	64.2	65.7	64.7	65.9	64.9	66.3
Albany	14174000	62.6	61.0	61.6	60.1	61.6	61.5	64.2
Salem	14191000	64.2	60.8	59.5	57.0	58.0	59.1	61.5
Newberg	14197900	62.6	59.5	58.1	55.8	56.0	56.6	58.5
Willamette Falls	14207740	69.7	67.4	66.8	65.4	65.1	65.2	66.0
				2016				
Owosso Bridge	14158100	82.9	86.8	82.6	81.3	82.2	83.0	83.8
Harrisburg	14166000	70.3	71.8	69.5	67.9	68.0	65.8	70.8
Albany	14174000	68.2	68.3	65.1	62.7	61.9	60.9	68.0
Salem	14191000	68.8	66.6	63.7	60.3	58.3	59.5	72.6
Newberg	14197900	66.6	64.2	61.8	58.9	56.6	57.5	69.9
Willamette Falls	14207740	70.9	69.2	68.4	67.4	65.6	65.8	74.8

Dimensionless Numbers and Useful Ratios

The information and concepts revealed thus far through the tracking of the quantity and age of water and heat from various sources may be sufficient to understand the interplay between upstream water and heat releases and the resulting mixture of water and heat sources at downstream locations in the Willamette River system. Additional insights into the heat budgets of river systems, the relative importance of different sources of heat to rivers, and the time required for certain processes to become important, however, can be gained through a more-detailed examination of heat-flux processes in stream systems. Several ratios and dimensionless numbers can help to provide a more thorough understanding of heat budgets and stream temperatures in the Willamette River system.

Heat Replacement Time Scale

A Heat Replacement Time Scale (HRTS) may be defined as the heat content of water in the river at a particular location divided by the incoming EEF across the water surface. Because the EEF is a rate in units of energy per time and heat content has units of energy, the HRTS has units of time and can be thought of as the time required for the incoming accumulated EEF to equal, or potentially replace, the existing heat content of water at a particular location. Relying on parts of equations 1 and 3, the HRTS can be expressed as:

$$HRTS = \frac{\rho V C_p T_w}{86400\, A\, (H_s - H_{sr} + H_a + H_{ei} + H_{ci})}$$

$$= \frac{\rho\, d_m C_p T_w}{86400\, (H_s - H_{sr} + H_a + H_{ei} + H_{ci})} \qquad (10)$$

where

$HRTS$ is the Heat Replacement Time Scale in days,

ρ is the density of water in kilograms per cubic meter (about 1,000),

V is the volume of water in cubic meters,

C_p is the specific heat of water (4,186 Joules per kilogram per degree Celsius),

T_w is the water temperature in degrees Celsius,

A is the surface area of the river reach of interest in square meters,

H_s is the incident energy flux from short-wave solar radiation in Joules per square meter per second,

H_{sr} is the reflected energy flux of short-wave solar radiation in Joules per square meter per second,

H_a is the incoming energy flux from long-wave atmospheric radiation in Joules per square meter per second,

H_{ei} is the incoming energy flux caused by condensation (if any) in Joules per square meter per second,

H_{ci} is the incoming energy flux from conduction (if any) across the air/water interface in Joules per square meter per second, and

d_m is the mean water depth in meters.

Clearly, the HRTS depends on many factors that vary over space and time, such as day/night cycles, weather variations, and the depths, shading, and water temperature of different river reaches. In this study, the HRTS is defined and used as a daily mean value, thus eliminating variations caused by day/night cycles at a single site. Water moving downstream will continually move through reaches with different HRTS values. If conditions did not vary, then the HRTS would represent a time period over which the influence of upstream heat sources on the temperature of a water parcel of interest would be substantially diminished. In other words, if the HRTS were constant as water moved downstream from a dam release, then the influence of incoming EEFs on the temperature of that water would become more important than the influence of upstream dam-release temperatures after a length of time equal to the HRTS had elapsed.

Some spatial and temporal patterns in the computed value of the HRTS are expected because of known variations in river depth and seasonal patterns in streamflow, water temperature, and weather conditions. For example, the Willamette River is much deeper in the pooled reach between Newberg and Willamette Falls than at most locations upstream of Newberg, and that greater depth increases the heat content and the resulting HRTS (fig. 12*A*). At Newberg, the HRTS is close to two weeks (14 days) during most of the simulation period in 2015, whereas the HRTS is roughly 2 to 3 days at Owosso Bridge, Harrisburg, and Salem, and about 5 days at Albany. Compared to summer, higher flows in late spring translate to greater mean depths, which would tend to increase the HRTS, but that increase would be partially offset by springtime water temperatures that tend to be cooler than those in summer, which would in turn decrease the heat content and the HRTS. Long, sunny days in mid-summer have large EEFs, which would tend to decrease the HRTS, but that decrease would be partially offset by the warm water temperatures during summer, which would increase the heat content and increase the HRTS. Although these variations in depth, temperature, and weather conditions do result in an apparent seasonal pattern in the HRTS (fig. 12*B*), it appears that mean depth is a more important influence than seasonality on the HRTS in the Willamette River system.

Although the concept of an HRTS provides some insights into the amount of time that must elapse before the heat content attributable to upstream dam releases diminishes to some small percentage, the HRTS is perhaps most useful when compared to the time required for water to move through the river system. The modeled age of water (and heat) sourced from upstream dam releases is a good measure of the average travel time of water through the Willamette River system; therefore, the ratio of the modeled age of water from upstream dam releases to the modeled HRTS provides a useful dimensionless comparison. When that ratio is equal to or greater than 1.0, it means that water from upstream dams was released long ago, relative to the HRTS. At locations and times when that ratio is more than 1.0, then, sufficient time has elapsed for most of the heat from upstream dam releases to be replaced by heat from other sources (such as EEFs) and the river temperature is likely to be less influenced by upstream dam-release temperatures. In the Willamette River, an analysis of this ratio is not straightforward because the HRTS is a strong function of river depth, and water traveling downstream is exposed to a range of potential HRTS conditions as that water traverses reaches with varying depths. Near the upstream WVP dams, the HRTS is often less than 2 to 3 days, but the travel time from those dams is far less, causing the ratio of age-of-water-from-dams to HRTS to be small (fig. 13). Farther downstream in the Willamette River, between the Santiam River confluence and Newberg, the age of water from upstream dam releases (in the range of 2 to 4 days in the summer of 2015) is closer to the range of HRTS values computed for that reach and upstream, and the ratio of age-of-water-from-dams to HRTS often is more than 0.5 (the orange to red colors in fig. 13*C*), indicating that sufficient time has elapsed for much of the heat from upstream dam releases to be replaced by heat from other sources. Downstream of Newberg, the computed HRTS is larger because of increased river depth, but water entering that reach from upstream has already had most of its dam-sourced heat replaced by heat from other sources, so the small ratio of age-of-water-from-dams to HRTS in that reach is less meaningful. Despite the highly variable HRTS in different reaches of the Willamette River system, this time scale is useful in developing an understanding of the transient nature of heat in river systems and the fact that more-downstream locations such as Salem and Newberg are largely unaffected

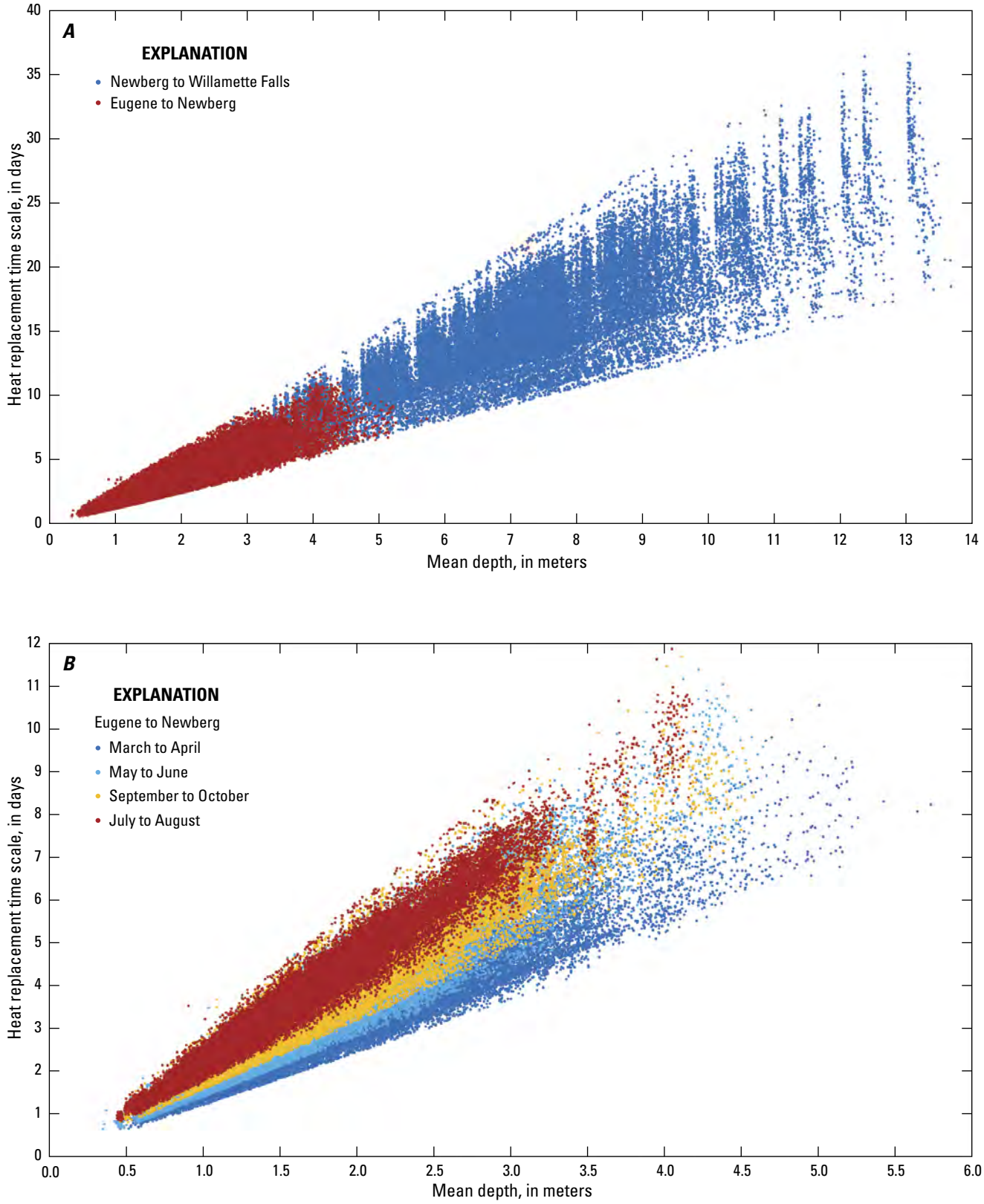

Figure 12. Heat Replacement Time Scale (HRTS) as a function of mean river depth showing that (*A*) the deeper river reaches downstream of Newberg have a longer HRTS, and (*B*) the HRTS varies slightly over time as water temperature and weather conditions change, Willamette River, northwestern Oregon, late March–October 2015.

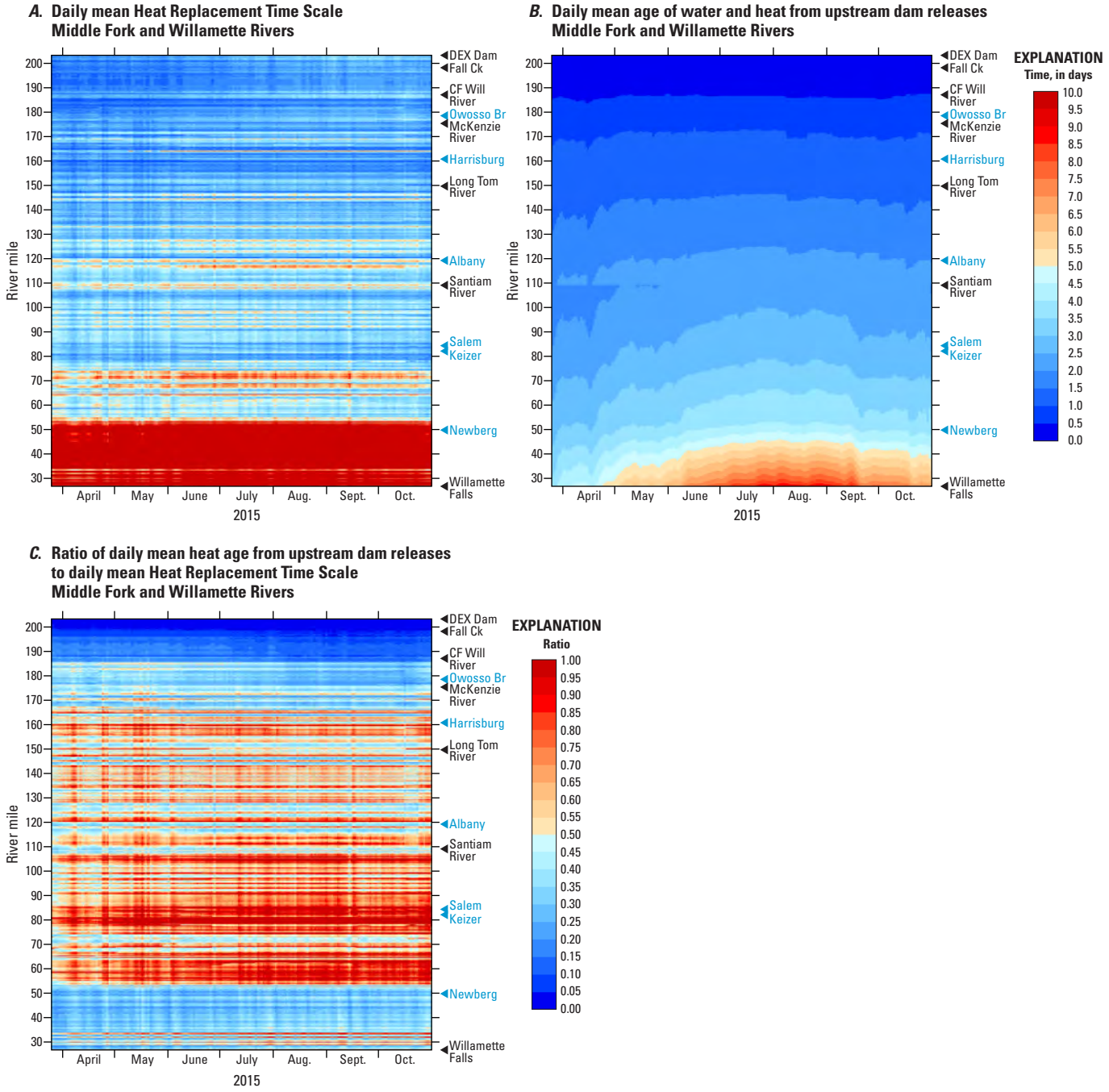

Figure 13. The (*A*) daily mean Heat Replacement Time Scale, (*B*) daily mean age of water and heat from upstream dam releases, and (*C*) ratio of the daily mean age of heat from upstream dam releases to the daily mean Heat Replacement Time Scale, Middle Fork Willamette and Willamette Rivers, northwestern Oregon, late March–October 2015. Abbreviations: DEX, Dexter Dam; Ck, Creek; CF, Coast Fork; Br, Bridge; Will, Willamette. Annotated locations in blue are measurement stations; those in black are tributaries or model boundaries.

by the temperature of upstream dam releases. The dam-release temperatures still have an effect on more-upstream sites such as Owosso Bridge and Harrisburg, but those effects are diminished at sites farther downstream, such as Albany and Keizer. As previously quantified by Rounds (2010), the augmented flow from dam releases still has an effect on temperatures occurring at the more-downstream sites, but the temperature of the water released from those dams is important only in reaches closer to the dams.

Ratio of Advective Heat Flux to Incoming Environmental Energy Flux

Water temperature in a river is affected by many processes, but the largest groups of heat-flux processes are advective and environmental, whereby advective processes transport or introduce heat through the movement or addition of water, and environmental energy fluxes transfer heat across river boundaries mostly through radiative processes, evaporation/condensation, and conduction. In stagnant water or in a moving reference frame in the absence of new sources of water, environmental heat fluxes would dominate the heat budget, but advective heat fluxes may be foremost in the heat budget of a flowing river at a fixed location. The ratio of the downstream advective heat flux to the incoming EEF across the water surface provides a useful comparison of the magnitude of the heat fluxes of these groups. Downstream advective heat fluxes increase with increasing streamflow and warmer water, whereas the amount of incoming EEF increases with increasing surface width, longer days, and increased sunshine. In the Willamette River system, the ratio of the downstream advective heat flux to the incoming EEF is large everywhere, with a magnitude ranging from about 100 to 6,000 or more during the March through October model simulation periods of 2011, 2015, and 2016 (fig. 14). Clearly, the best predictor of water temperature at any location in the main, well-mixed channels of the Willamette River network is the water temperature just upstream. Given enough time and downstream distance, the influence of accumulated EEFs becomes important, but the instantaneous ratio of advective and environmental heat fluxes shows that advection is a dominant process in the heat budget at any fixed location in the Willamette River.

Environmental Energy Flux Ratio

Another ratio that may be suggested by an examination of stream heat budgets is the ratio of incoming to outgoing EEFs across the water surface. That ratio— here called EEFR—is an indicator of whether a waterbody is likely to be warming or cooling, and would be expected to vary greatly over the course of the day because short-wave solar radiation is a major component of the incoming EEF and is nonzero only during daylight. The EEFR is defined as:

$$EEFR = \frac{H_s - H_{sr} + H_a + H_{ei} + H_{ci}}{H_b + H_{eo} + H_{co}} \qquad (11)$$

where

$EEFR$ is the environmental energy flux ratio (dimensionless),
H_s is the incident energy flux from short-wave solar radiation,
H_{sr} is the reflected energy flux of short-wave solar radiation,
H_a is the incoming energy flux from long-wave atmospheric radiation,
H_{ei} is the incoming energy flux caused by condensation (if any),
H_{ci} is the incoming energy flux from conduction (if any) across the water surface,
H_b is the outgoing energy flux from long-wave back radiation,
H_{eo} is the outgoing energy flux caused by evaporation (if any), and
H_{co} is the outgoing energy flux from conduction (if any) across the water surface.

The daily mean EEFR provides an overall indication of warming or cooling over the course of the day.

Spatial and temporal patterns in the EEFR tend to reflect general patterns in water temperature and the imposed weather conditions because EEFR is not a function of river width or depth but is dependent on water temperature and weather conditions such as air temperature, solar insolation, cloudiness, wind speed, and relative humidity. When river temperature is cooler than the temperature it would have when at equilibrium with the imposed EEFs, the EEFR would indicate a tendency towards warming with a value greater than 1.0. Similarly, when river temperature is warmer than its equilibrium temperature, the EEFR would indicate a tendency towards cooling with a value less than 1.0 (fig. 15). During June of 2015, when air temperatures were abnormally hot, water released from Dexter Dam was cooler than what would be in equilibrium with those weather conditions, so the EEFR in the Middle Fork Willamette River downstream of Dexter Dam was well above 1.0. In contrast, during September and October of 2015, releases from Dexter Dam generally were warmer than the environmental equilibrium temperature, as evidenced by an EEFR that often was less than 1.0. When river temperatures were relatively cool and the weather was warm, such as the more-upstream reaches of the Willamette River for most of the March-October simulation period, the EEFR indicated strong warming (values greater than 1.0 plotted as orange to red colors in fig. 15). Farther downstream, after the river was warmed by an influx of heat from the surrounding environment, the EEFR tended to vary more closely around 1.0, with variations depending on the weather. The EEFR is a relatively simple quantity to compute, and may be one of the simplest means to indicate warming or cooling based only on the weather and the current river temperature, particularly when visualized with a time/distance color map over an entire model domain and a range of dates.

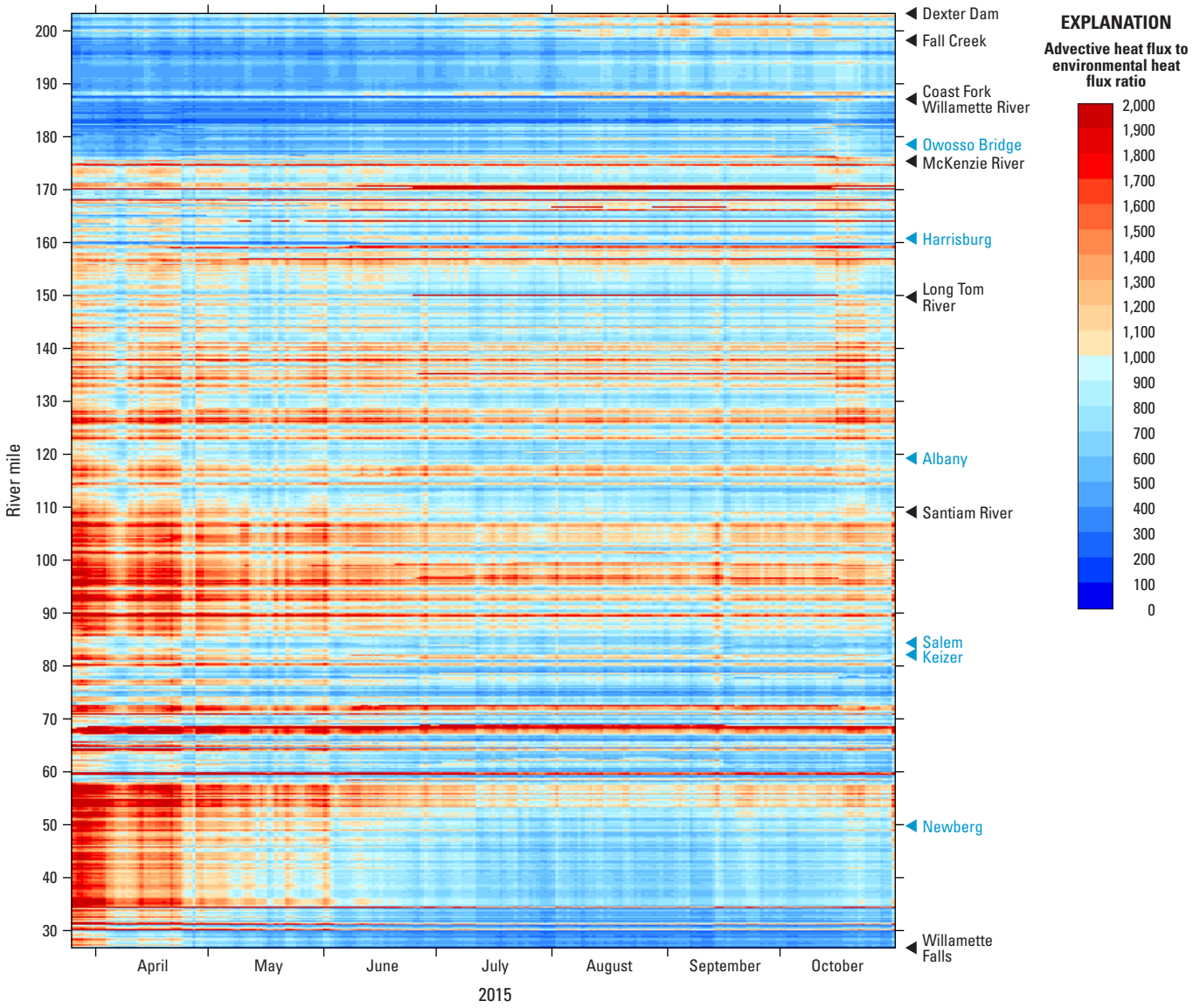

Figure 14. Daily mean ratio of the downstream advective heat flux to the incoming environmental energy flux across the water surface, Middle Fork Willamette and Willamette Rivers, northwestern Oregon, late March–October 2015. Annotated locations in blue are measurement stations; those in black are tributaries or model boundaries.

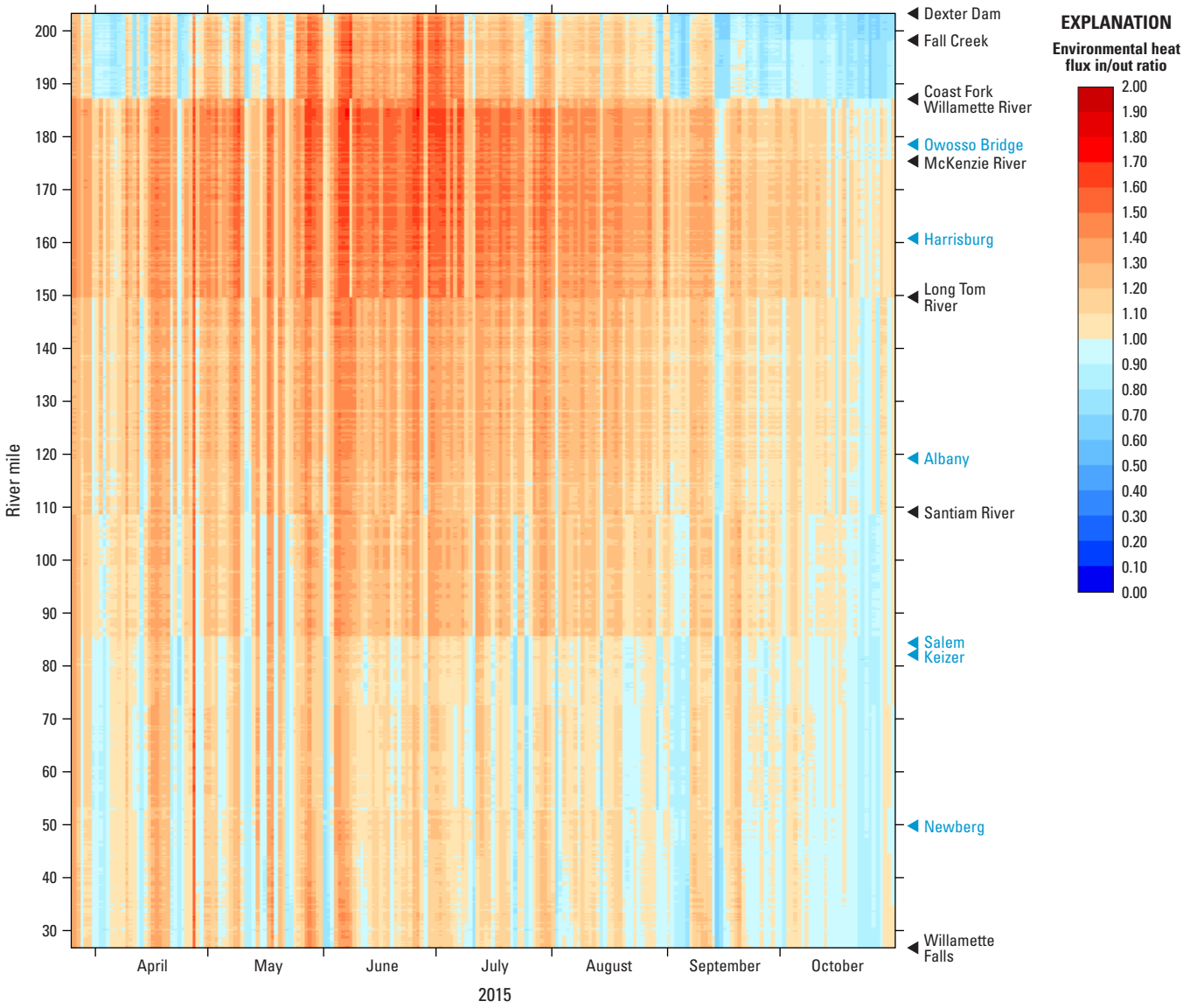

Figure 15. Daily mean ratio of the incoming and outgoing environmental energy fluxes across the water surface, Middle Fork Willamette and Willamette Rivers, northwestern Oregon, March–October 2015. Annotated locations in blue are measurement stations; those in black are tributaries or model boundaries.

A Flow-Augmentation Case Study

A case study provides an excellent means of illustrating how flow augmentation can affect downstream water temperature and also provides a good baseline for a comparative analysis of how such a change in flow might alter the distribution of heat sources at downstream sites. In August of 2017, an abnormally large volume of water was intentionally released from Dexter Dam (and multiple reservoirs upstream) on the Middle Fork Willamette River in an effort to decrease downstream water temperatures and thereby improve fish habitat. An analysis of this measured flow increase in 2017, combined with an assessment of a hypothetical modeled flow increase of similar magnitude in 2016, shows that increased flow extends the heat signature from dams farther downstream and that the actual thermal effect on downstream locations is highly dependent on the temperature of dam releases.

From early August through early September of 2017, releases from Dexter Dam on the Middle Fork Willamette River were substantially higher than the typical release rates for that time period. On August 1–2, 2017, releases from Dexter Dam were increased from roughly 1,550 to 3,700 ft^3/s (Middle Fork Willamette River near Dexter, USGS site 14150000), an increase of about 2,150 ft^3/s that was corroborated by a measured increase in streamflow from 1,850 to 4,250 ft^3/s, an increase of 2,400 ft^3/s, from a second streamgaging station downstream (Middle Fork Willamette River at Jasper, USGS site 14152000). At

several streamgaging stations farther downstream along the Willamette River (Harrisburg [USGS site 14166000], Corvallis [USGS site 14171600], and Albany [USGS site 14174000]), the measured increase in streamflow was closer to 3,000 ft³/s (fig. 16*A*).

This large increase in flow during August 2017 had different effects on the measured water temperature, depending on the downstream location. Not far downstream from Dexter Dam, at the Dexter and Jasper gaging stations, the effect was manifested mainly as a decrease in the daily temperature range, which is consistent with a larger thermal mass diluting similar EEF inputs (fig. 16*B*). Farther downstream and as far downstream as Newberg, however, the increased flow caused river temperatures to decrease compared to late-July conditions, even as upstream temperatures were rising because of higher release temperatures at Dexter Dam. Measured water temperatures at Harrisburg and Albany appear to have decreased by about 1.5 °C or more by the second week of August (fig. 16*B*). The amount of warming that occurred from Dexter downstream to Newberg later in the month was

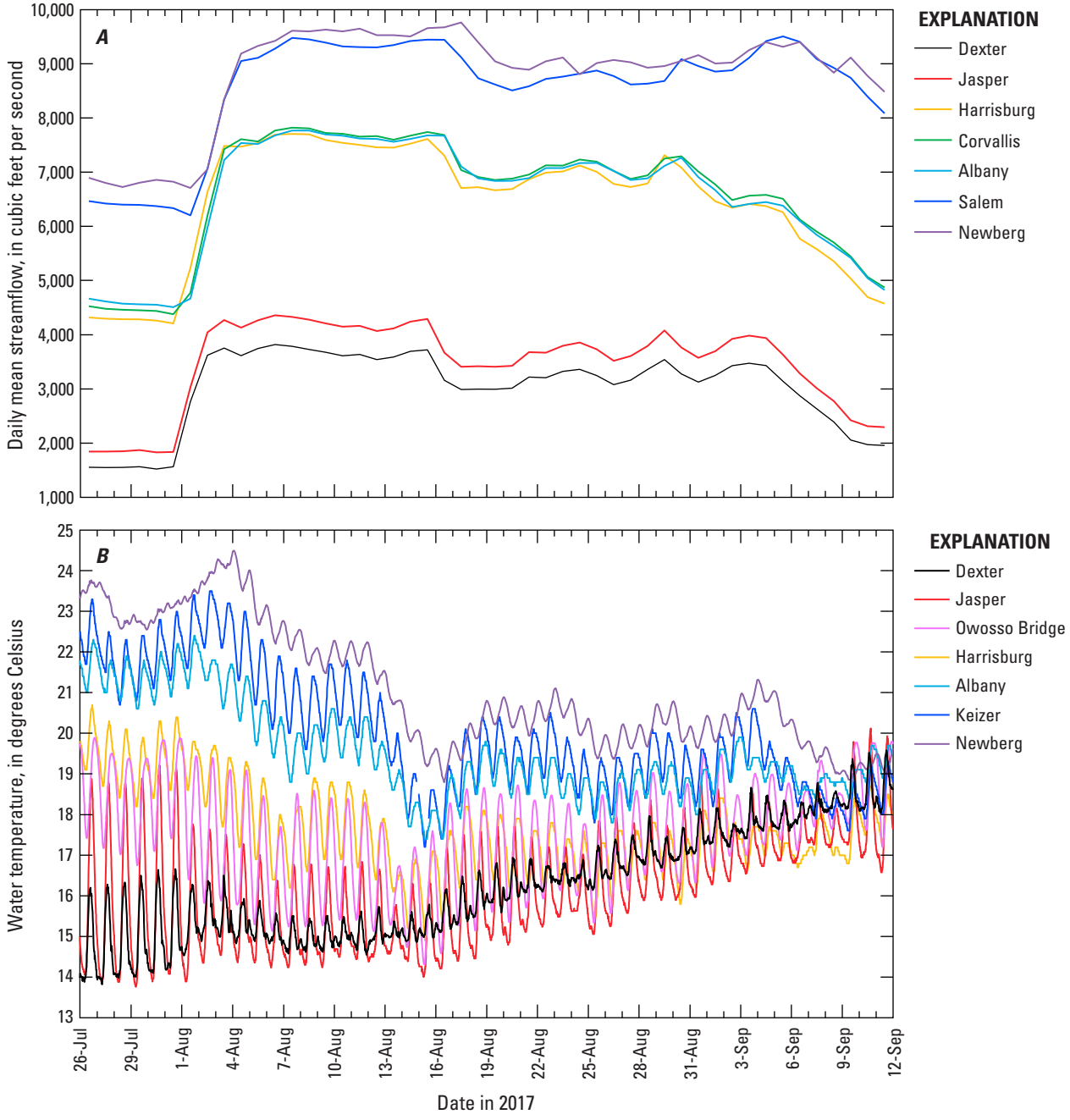

Figure 16. The (*A*) daily mean streamflow and (*B*) subdaily water temperature for a period of elevated water releases from Dexter Dam at selected locations in the Middle Fork Willamette and Willamette Rivers, northwestern Oregon, August 2017.

clearly diminished, from an increase of as much as 8 °C in late July to 3 °C or less in late August and early September. Many factors probably contributed to the decreased warming in August. Shorter days later in the month and smoke from regional forest fires, along with periodic cloudy weather (particularly August 13–15), would have decreased energy inputs from short-wave solar radiation. The increased streamflow, however, undoubtedly resulted in decreased travel time (less time for warming by EEFs) and greater thermal mass to resist warming. Given the modeling results from this study, it is highly likely that the increased streamflow was an important causal factor for the decreased amount of warming at downstream sites.

As a check on the general magnitude of the decreased warming, the regression models of Stratton Garvin and others (2022b) were used to estimate the change in the 7-day average of the daily mean (7dADMean) water temperature that might be caused by a hypothetical increase in streamflow at Albany of 3,000 ft^3/s during August of 2017. Regression model results showed that 7dADMean water temperatures might be expected to decrease by somewhere in the range of 0.9 to 2.3 °C, depending on air temperature, which is consistent with the measured decrease of about 1.5 °C. The regression models are based only on historical data and do not track water through the river system or take into account any change in upstream conditions, but the results are still useful in corroborating a certain amount of expected cooling caused by a substantial increase in streamflow. Stratton Garvin and Rounds (2022a) used CE-QUAL-W2 model simulations to confirm that flow augmentation of about 1,000 ft^3/s from upstream dam releases can result in a small amount of cooling in downstream reaches of the Willamette River. The simulated cooling was typically small, but as much as 0.8 °C for the average July water temperature downstream of the Santiam River confluence, and as much as 1.7 °C for the daily maximum water temperature downstream of the Santiam River confluence.

A change in Willamette River water temperature in response to a large increase in streamflow also was tested with the models used in this study. Superimposed on measured conditions from 2016 (because 2017 was not among the years modeled in this study), the 2016 modeled releases from Dexter Dam on the Middle Fork Willamette River were hypothetically increased by 2,500 ft^3/s (70.79 m^3/s) during the month of August (days 214–244) while keeping all other 2016 conditions unchanged (including 2016 dam-release temperatures), and downstream simulated water temperatures were compared to those resulting from unmodified flow conditions. Prior to the flow increase, releases from Dexter Dam in late July of 2016 were about 1,660 ft^3/s (about 47 m^3/s), and in early September the releases were approximately 1,340 ft^3/s (about 38 m^3/s); therefore, this hypothetical flow increase during August was substantial, causing streamflow in the Middle Fork Willamette River to increase by more than a factor of 2.5. This level of flow augmentation is certainly possible, as a similar level of augmentation occurred in August of 2017, but it requires a large amount of water to be released from upstream reservoirs. A flow increase of 2,500 ft^3/s requires an additional 4,959 acre-ft of water per day, and 153,719 acre-ft over the course of 31 days—well less than the full-pool storage capacities of Lookout Point Lake (455,800 acre-ft) and Hills Creek Lake (355,500 acre-ft) on the Middle Fork Willamette River upstream of Dexter Lake and Dexter Dam, but still a substantial fraction of their total storage capacity.

Downstream of Dexter Dam, the simulation of an extra 2,500 ft^3/s in streamflow showed both increases and decreases in water temperature. At sites close enough to Dexter Dam for the river to retain a substantial fraction of heat content from that upstream dam release (Jasper, Owosso Bridge, and Harrisburg, for example), the flow augmentation during August caused the river to become slightly warmer, whereas a slight overall cooling effect was predicted at sites farther downstream (fig. 17). The warming near the dam as compared to baseline 2016 conditions was caused by the fact that the temperature of the August releases (measured and modeled) from Dexter Dam in 2016 were in the range of 18 to 21 °C rather than the 15 to 18 °C (measured) releases that occurred in August of 2017, and 18 to 21 °C was a bit warmer than water inputs from Fall Creek or the McKenzie River at that time. Many factors could account for the warmer releases from Dexter Dam in 2016 compared to those in August 2017, including weather conditions, upstream reservoir temperatures, or dam operations, but an analysis of those factors was beyond the scope of this study. Regardless, these hypothetical simulations for 2016 showed that any cooling in downstream reaches caused by a decrease in travel time and an increase in thermal mass took longer to manifest and did not generally occur in the simulation results until the water had travelled downstream at least as far as Corvallis. The cooling was maximized in the river reach near Albany, upstream of the Santiam River confluence where a substantial amount of dilution occurred. Still, the cooling effect continued downstream to and past Newberg. The amount of warming (near the dam) and cooling (farther downstream) was of approximately similar magnitude in this hypothetical modeling experiment for August of 2016—within ±1.0 °C in either direction for the 7dADMean (fig. 17). A time/distance color map illustrates this effect across the entire model domain, with the cooling maximized just upstream of the Santiam River confluence and more prevalent at downstream locations (fig. 18). It is logical to conclude that the cooling effect would have been more prevalent and of higher magnitude in August of 2017 because of the colder releases from Dexter Dam in 2017 relative to 2016.

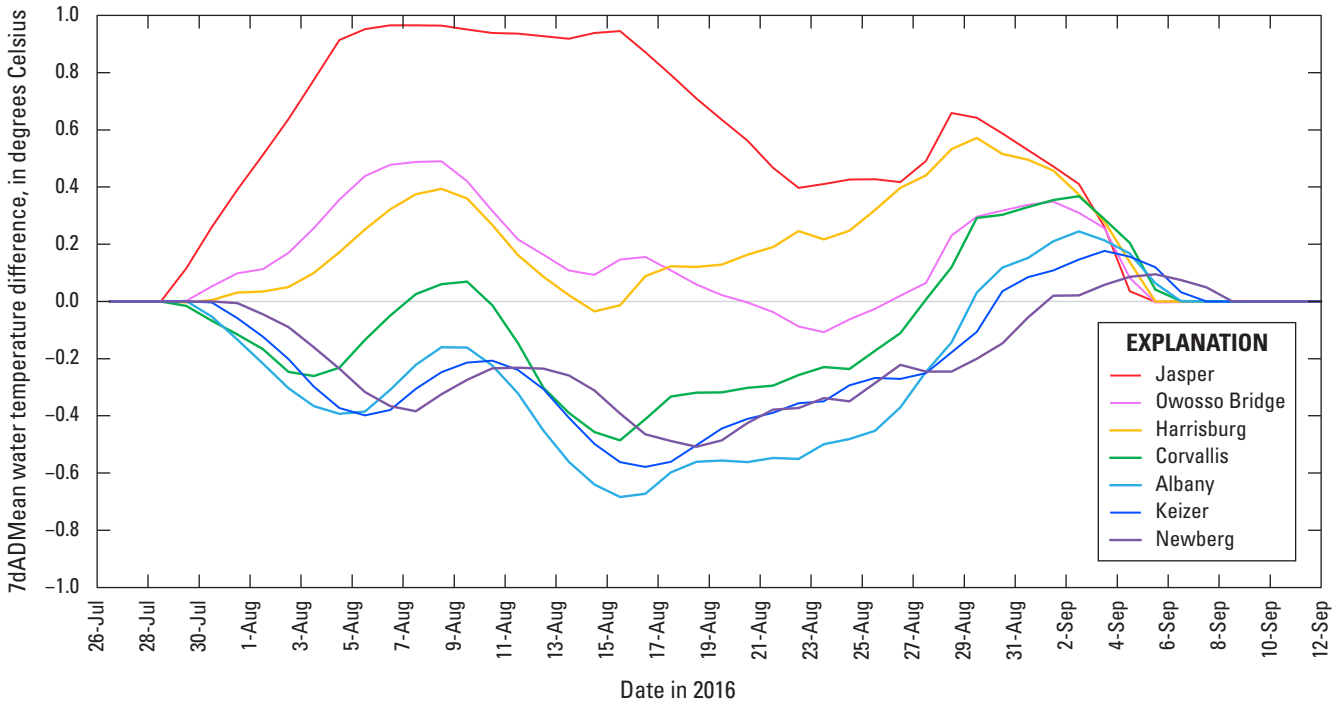

Figure 17. Change in the modeled 7-day average of the daily mean water temperature (7dADMean) at sites in the Middle Fork Willamette and Willamette Rivers caused by a hypothetical increase of 2,500 cubic feet per second in the release rate of water from Dexter Dam, Middle Fork Willamette River, northwestern Oregon, August 2016. Sites are listed from upstream to downstream.

In addition to modifying downstream river temperatures, the hypothetical 2,500 ft^3/s increase in flow as simulated from Dexter Dam during August of 2016 also caused a shift in the distribution of heat sources at downstream sites. The heat attributable to upstream dam releases was substantially increased during August at downstream sites (figs. 19*A* and *C*), and the heat attributable to EEFs was decreased (figs. 19*B* and *D*). At Harrisburg, the average percentage of heat sourced from upstream dams during August was 32 percent for the baseline model run, but 52 percent for the flow-augmentation scenario, which was accompanied by a decrease from 52 to 37 percent for the heat sourced from EEFs. The Harrisburg site was far enough upstream that the extra releases from Dexter Dam, which were warmer than the temperatures of other tributaries at that time, resulted in warming. The greatest cooling in this flow-augmentation scenario was manifested in the river reach downstream of Albany and upstream of the Santiam River confluence (fig. 18). At Albany, the average percentage of heat sourced from upstream dams in August was 20 percent for the baseline model run and 38 percent from the flow-augmentation scenario, whereas the heat sourced from EEFs decreased from 65 to 51 percent. The travel time from Dexter Dam to Albany decreased from a mean of 1.8 days in August for the baseline model run to 1.4 days during the flow-augmentation scenario. Although a decrease in the time of exposure of the river to EEFs of 0.4 days likely contributed to decreased warming at Albany, the increase in thermal mass of roughly 2,500 ft^3/s was probably more important in resisting an increase in river temperature.

Clearly, the effects of a large increase in flow from upstream dams extends the thermal effects from those dams farther downstream, as evidenced by simulation results showing the increased influence of dam releases on downstream heat content and the decreased influence of EEFs, but the actual thermal effects on water temperature are highly dependent on the release temperatures. In this hypothetical case for August of 2016, releases from Dexter Dam were warmer than temperatures in nearby tributaries such as Fall Creek and the McKenzie River, causing warming near the dam. Much farther downstream, the decreased travel time and increased thermal mass resulted in cooling (fig. 18). Consequently, the effects of hypothetical flow-management strategies on water temperature are best informed by a two-pronged approach in which an analysis of modeled temperatures is used to evaluate the direct downstream thermal effects, and an analysis of the distribution of heat sources is used to evaluate the relative influence of release temperatures (heat from upstream dam releases) versus the downstream influence of EEFs, travel time (age), and thermal mass. A straightforward temperature modeling exercise is adequate for quantifying the downstream thermal effects, but an analysis of the distribution of heat sources and travel times will provide additional insights into the reasons for the downstream thermal changes.

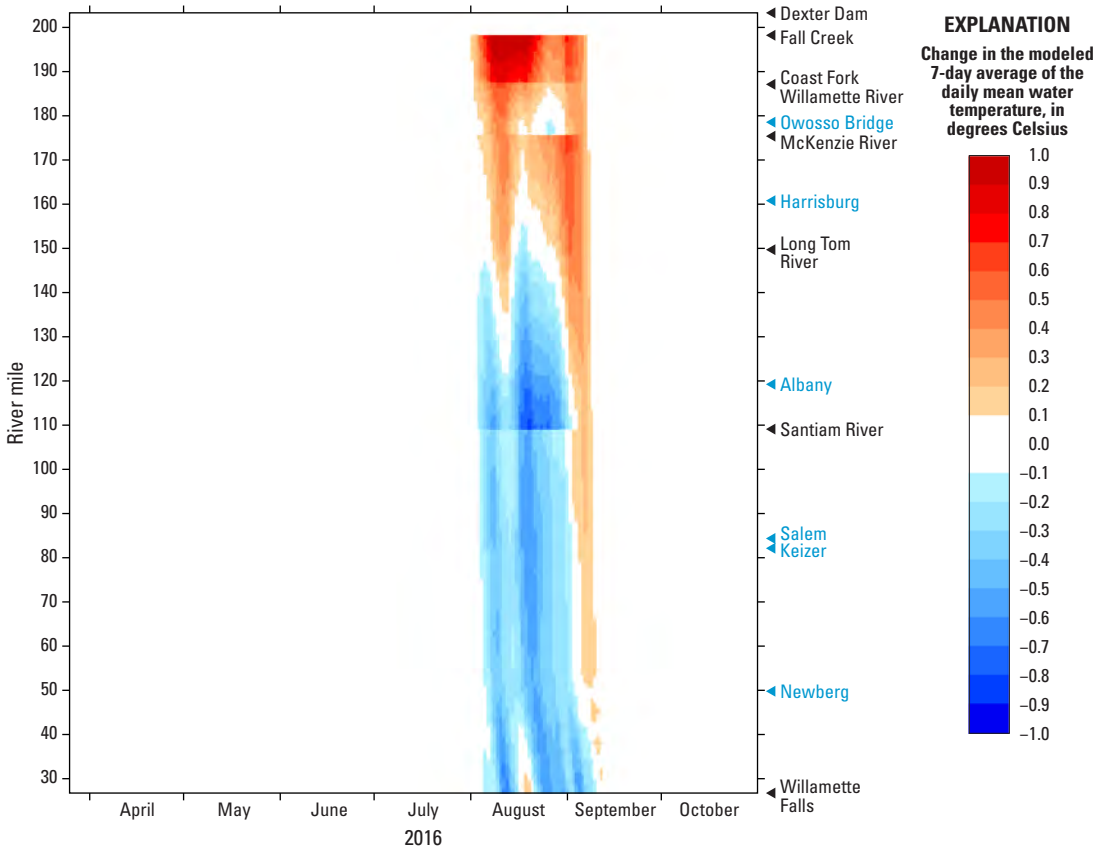

Figure 18. Late March through October 2016 change in the modeled 7-day average of the daily mean water temperature caused by a hypothetical increase of 2,500 cubic feet per second in the release rate of water during August of 2016 from Dexter Dam, Middle Fork Willamette River, northwestern Oregon. Annotated locations in blue are measurement stations; those in black are tributaries or model boundaries.

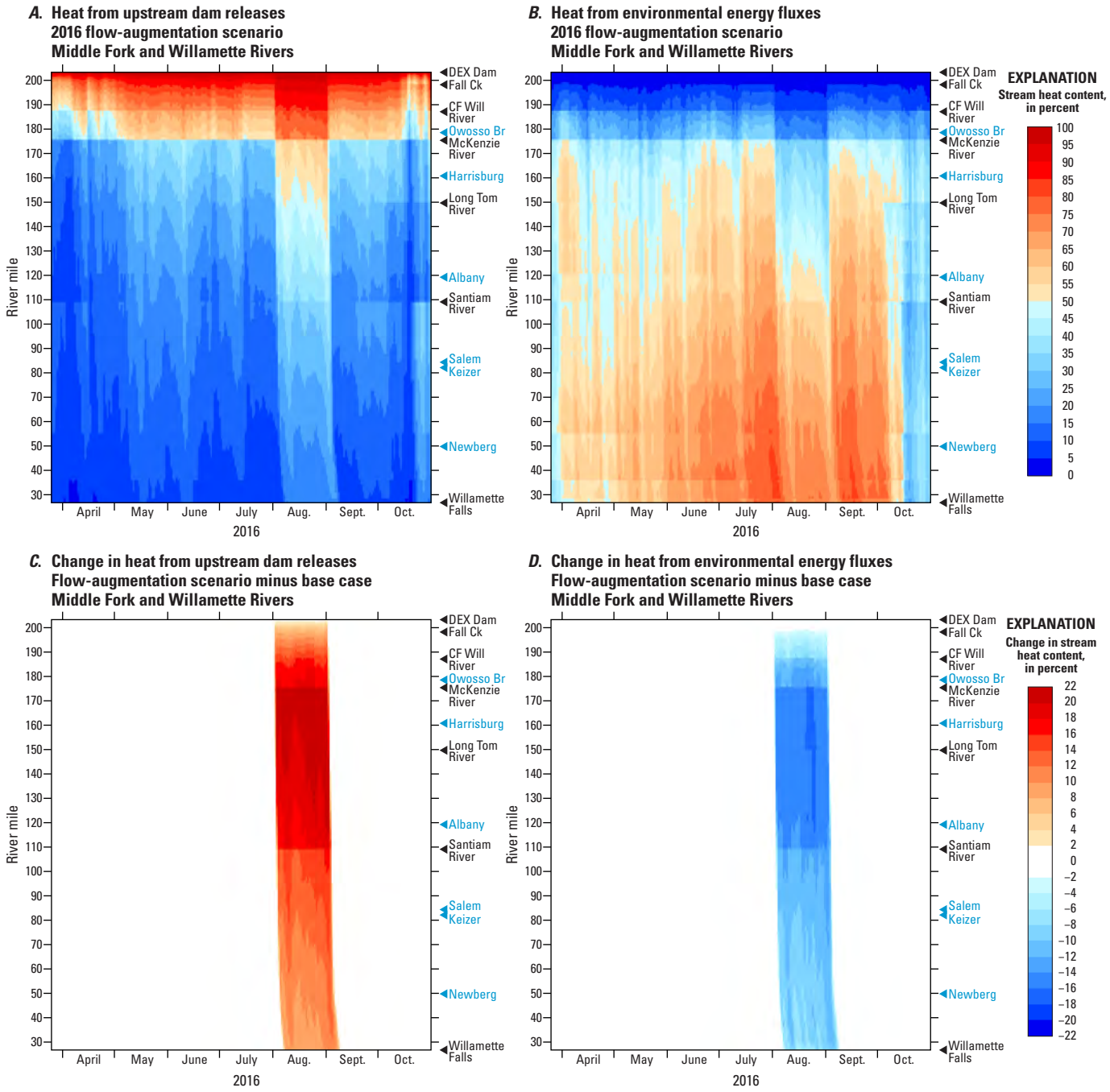

Figure 19. Late March through October 2016 percentage of stream heat content attributable to (*A*) upstream dam releases and (*B*) environmental energy fluxes for the flow-augmentation scenario, and the change in the percentage of stream heat content attributable to (*C*) upstream dam releases and (*D*) environmental energy fluxes caused by a hypothetical increase of 2,500 cubic feet per second in the release rate of water during August of 2016 from Dexter Dam, Middle Fork Willamette River, northwestern Oregon. Abbreviations: DEX, Dexter Dam; Ck, Creek; CF, Coast Fork; Br, Bridge; Will, Willamette. Annotated locations in blue are measurement stations; those in black are tributaries or model boundaries.

Summary and Implications for Monitoring and Management

This study of the Willamette River system shows how the development and use of modeling tools can reveal critical facts regarding stream heat budgets and heat sources, as well as the response of streams to weather and flow conditions, river morphology (width, depth), and riparian characteristics (shade). Water temperature in rivers is the result of the interaction of many physical and meteorological factors, all of which can be reasonably and accurately simulated in models, leading to the following conclusions:

- The largest incoming and outgoing energy fluxes across the surface of the Willamette River are confirmed by model simulation results to be radiative, including short-wave solar radiation, long-wave atmospheric radiation, and long-wave back radiation. The next most important component of the energy budget is evaporation, whereas conductive heat transfer typically is a minor component for large rivers such as the Willamette River. Cloud cover (or smoke) and riparian or topographic shading is important because it blocks some of the short-wave solar radiation.

- Deep river reaches have more heat capacity (thermal mass) than shallow rivers of similar width to resist changes in water temperature caused by environmental energy fluxes (EEFs) and other heat inputs.

- In river reaches just downstream of dams, water temperature is greatly affected by the temperature of those dam releases. Farther downstream, EEFs and other sources of heat become increasingly important in determining river temperature, thereby diminishing the fraction of heat in the river that can be attributed directly to upstream dam releases.

- In the Willamette River downstream of the McKenzie River, approximately half of the water in the river during late summer can be tracked back to upstream dam releases under current flow-management practices, but less than half of the heat content in the river can be attributed to upstream dam releases. Upstream dam releases account for approximately 57 to 59 percent of the heat content in the river in August of 2011, 2015, and 2016 at Owosso Bridge in Eugene (upstream of the McKenzie River confluence), but only 26 to 32 percent at Harrisburg and decreasing amounts as the water moves downstream: 12 to 13 percent at Keizer and about 9 percent at Newberg. Even after accounting for dilution, only 22 to 24 percent of the heat content in the river at Keizer in August can be attributed to upstream dam releases.

- EEFs account for approximately 52 to 54 percent of the heat content in the river in August of 2011, 2015, and 2016 at Harrisburg, increasing to 69 to 73 percent at Keizer and 75 to 79 percent at Newberg as the water moves downstream.

- After some amount of time elapses from the point at which water is released from upstream dams and begins moving downstream—often about 2 to 3 days in the Willamette River system during summer—the influence of upstream dam-release temperatures is largely erased and the heat content attributable to those dam releases becomes small. The choice of a criterion is somewhat arbitrary, but results from this study show that the heat content derived from upstream dam releases during summer diminishes to less than 10 percent at some point downstream of Keizer, at which point the temperature of the river is dominated by factors such as river width and depth, streamflow, and weather conditions (EEFs).

- The amount of time that would be required for incoming EEFs across the water surface to replace all of the heat content in the Willamette River varies with river width and depth, water temperature, and weather conditions, but commonly is less than 5 days at most locations upstream of Newberg during summer. Reaches or locations with deeper water have more heat capacity and therefore more time would be required for incoming EEFs to replace the greater heat content.

The results of this study are important for developing a better understanding of riverine thermal conditions and for informing the flow- and temperature-management strategies of water-resource managers and agencies, particularly in basins with large upstream reservoirs like the Willamette River Basin. As operators of the 13 dams of the Willamette Valley Project (WVP), the U.S. Army Corps of Engineers can directly control the temperature of river reaches just downstream of several WVP dams during summer through the strategic selection and use of dam outlets that affect the temperature of water releases. Farther downstream, however, water temperature is largely subject to weather conditions, the thermal mass of the river, and the amount of time available for EEFs to replace some of the river heat content. At such downstream sites, upstream dam releases are still important in terms of their effect on streamflow, but the ability of dam operators to influence downstream temperatures greatly diminishes after 2 to 3 days of travel time from those upstream dams. This study showed that the average age of water released from WVP dams in late summer (August) is approximately 1.9 to 2.1 days at Albany, 2.6 to 2.8 days at Salem, 3.8 to 4.3 days at Newberg, and 6.7 to 8.8 days at Willamette Falls. The heat attributable to upstream dam releases diminishes with increasing downstream distance and travel time, and in late summer that percentage of dam-sourced heat is relatively small at sites two or more days downstream: 17 to 20 percent at Albany, 12 to 14 percent

at Salem and Keizer, about 9 percent at Newberg, and 6 to 7 percent at Willamette Falls, using simulation results from August of 2011, 2015, and 2016. Water temperature at sites far downstream of the WVP dams, therefore, is not particularly influenced by dam-release temperatures. If dam operators are to influence water temperature at those downstream sites, they must rely primarily on flow augmentation to decrease travel time and increase thermal mass in order to decrease the accumulating effect of EEFs that tend to warm the river in summer.

Large amounts of water released from upstream dams can have a measurable effect on water temperature in the Willamette River, even at sites far enough downstream that the actual heat content attributable to upstream dam releases is minimal. Indeed, results of simulations made with CE-QUAL-W2 models show that flow augmentation of about 1,000 cubic feet per second (ft^3/s) from upstream dam releases can decrease the average July water temperature in the Willamette River downstream of the Santiam River by up to 0.8 °C and can decrease daily maximum Willamette River temperatures downstream of the Santiam River by as much as 1.7 °C. This cooling is directly attributable to increased streamflow through decreased travel time and increased thermal mass; the former decreases the time available for EEFs to increase the heat content of the river, and the latter spreads the incoming heat over a larger mass of water, thereby decreasing the downstream rate of warming. A simple multiple linear regression model to estimate water temperature from streamflow and air temperature also predicts that a 1,000 ft^3/s increase in streamflow would cause a measurable decrease in water temperature at Willamette River sites. Depending on air temperature, the decrease ranges from 0.9 °C at Harrisburg and Albany to 0.7 °C at Keizer, as modeled for August of 2018.

A large amount of flow augmentation from upstream dam releases was shown in this study to substantially affect downstream temperatures and the magnitude of heat from various upstream sources at downstream sites. A hypothetical increase in releases from Dexter Dam on the Middle Fork Willamette River by 2,500 ft^3/s was modeled for the month of August in 2016 and compared to a similar flow increase that occurred in August of 2017. Both the modeled (2016) and measured (2017) effects were substantial at sites near the dam, and still measurable (more than a few tenths of a degree Celsius) even at sites 150 miles downstream of Dexter Dam (Newberg is about 154 miles downstream). Releases from Dexter Dam in August of 2017, however, were cooler than those modeled (and measured) for August of 2016, leading to different levels of cooling (2017) and warming (2016) in downstream river reaches within a day or so of travel time from Dexter Dam, but more consistent cooling at sites farther downstream in both years. Strategies to increase dam releases during summer for the benefit of downstream fish habitat, therefore, would benefit from associated actions to manage the temperature of those dam releases. The analysis of modeled heat sources in 2016 also showed that flow augmentation increased the direct downstream effects of dam releases on river heat content, with an increase of 20 percent at Harrisburg and 12 percent at Keizer, and with concomitant decreases in the influence of EEFs on river heat content. Even with such a high level of flow augmentation, however, the heat content attributable to EEFs was still more than 50 percent at and downstream of Albany and over 70 percent at Newberg.

Riverine heat budgets and environmental heat fluxes are controlled by the same processes all over the world, so a better understanding of the interplay of these processes in the Willamette River Basin should be illustrative of conditions occurring in similar river basins elsewhere. The information and insights gained as a result of this study, as well as the tools and models developed, should help water-resource managers to better understand the potential range of effects of flow- and temperature-management strategies, and thereby create and implement more effective responses to the demands of climate change and the management of habitat for endangered species.

Acknowledgments

The authors are thankful for useful discussions, insights, and information provided by Norman Buccola and Rich Piaskowski of the U.S. Army Corps of Engineers, Portland District. Thanks also are due to Krista Jones of the U.S. Geological Survey's Oregon Water Science Center for useful discussions and feedback on the figure portraying the energy fluxes entering and leaving stream systems.

References Cited

Annear, R.L., McKillip, M.L., Khan, S.J., Berger, C.J., and Wells, S.A., 2004a, Willamette River Basin temperature TMDL model—Boundary conditions and model setup: Portland, Oreg., Portland State University, Department of Civil and Environmental Engineering, Technical Report EWR-01-04, 530 p.

Annear, R.L., McKillip, M.L., Khan, S.J., Berger, C.J., and Wells, S.A., 2004b, Willamette River Basin temperature TMDL model—Model scenarios: Portland, Oreg., Portland State University, Department of Civil and Environmental Engineering, Technical Report EWR-03-04, 944 p.

Arora, R., Toffolon, M., Tockner, K., and Venohr, M., 2018, Thermal discontinuities along a lowland river—The importance of urban areas and lakes: Journal of Hydrology, v. 564, p. 811–823, accessed January 9, 2021, at https://doi.org/10.1016/j.jhydrol.2018.05.066.

Bartholow, J.M., 2000, The stream segment and stream network temperature models—A self-study course (version 2.0): U.S. Geological Survey Open-File Report 99–112, 276 p., accessed April 24, 2020, at https://doi.org/10.3133/ofr99112.

Berger, C.J., McKillip, M.L., Annear, R.L., Khan, S.J., and Wells, S.A., 2004, Willamette River Basin temperature TMDL model—Model calibration: Portland, Oreg., Portland State University, Department of Civil and Environmental Engineering, Technical Report EWR-02-04, 341 p.

Bloom, J.R., 2016, South Santiam River, Oregon—Hydrodynamics and water temperature modeling, 2000-2002: Portland, Oregon, Oregon Department of Environmental Quality, 53 p.

Bogan, T., Mohseni, O., and Stefan, H.G., 2003, Stream temperature-equilibrium temperature relationship: Water Resources Research, v. 39, no. 9, p. 1245, accessed January 9, 2021, at https://doi.org/10.1029/2003WR002034.

Brown, G.W., 1969, Predicting temperatures of small streams: Water Resources Research, v. 5, no. 1, p. 68–75, accessed January 9, 2021, at https://doi.org/10.1029/WR005i001p00068.

Buccola, N.L., Rounds, S.A., Sullivan, A.B., and Risley, J.C., 2012, Simulating potential structural and operational changes for Detroit Dam on the North Santiam River, Oregon, for downstream temperature management: U.S. Geological Survey Scientific Investigations Report 2012–5231, 68 p. [Also available at https://doi.org/10.3133/sir20125231.]

Buccola, N.L., 2017, Water temperature effects from simulated changes to dam operations and structures in the Middle and South Santiam Rivers, Oregon: U.S. Geological Survey Open-File Report 2017–1063, 19 p., accessed April 24, 2020, at https://doi.org/10.3133/ofr20171063.

Buccola, N.L., Stonewall, A.J., and Rounds, S.A., 2015, Simulations of a hypothetical temperature control structure at Detroit Dam on the North Santiam River, northwestern Oregon: U.S. Geological Survey Open-File Report 2015–1012, 30 p., accessed June 1, 2020, at https://doi.org/10.3133/ofr20151012.

Buccola, N.L., Stonewall, A.J., and Sullivan, A.B., Kim, Yoonhee, and Rounds, S.A., 2013, Development of CE-QUAL-W2 models for the Middle Fork Willamette and South Santiam Rivers, Oregon: U.S. Geological Survey Open-File Report 2013–1196, 55 p. [Also available at https://doi.org/10.3133/ofr20131186.]

Buccola, N.L., Turner, D.F., and Rounds, S.A., 2016, Water temperature effects from simulated dam operations and structures in the Middle Fork Willamette River, western Oregon: U.S. Geological Survey Open-File Report 2016–1159, 39 p., accessed April 24, 2020, at https://doi.org/10.3133/ofr20161159.

Caissie, D., 2006, The thermal regime of rivers—A review: Freshwater Biology, v. 51, no. 8, p. 1389–1406, accessed December 13, 2020, at https://doi.org/10.1111/j.1365-2427.2006.01597.x.

Costanzo, S., Kelsey, H., and Saxby, T., 2015, Willamette River report card 2015—Scores and scoring methodology: Integration & Application Network, University of Maryland Center for Environmental Science, accessed January 9, 2021, at https://ecoreportcard.org/report-cards/willamette-river/publications/2015-willamette-methods-report/.

Edinger, J.E., Duttweiler, D.W., and Geyer, J.C., 1968, The response of water temperatures to meteorological conditions: Water Resources Research, v. 4, no. 5, p. 1137–1143, accessed January 9, 2021, at https://doi.org/10.1029/WR004i005p01137.

Keefer, M.L., Taylor, G.A., Garletts, D.F., Gauthier, G.A., Pierce, T.M., and Caudill, C.C., 2010, Prespawn mortality in adult spring Chinook salmon outplanted above barrier dams: Ecology Freshwater Fish, v. 19, no. 3, p. 361–372, accessed January 9, 2021, at https://doi.org/10.1111/j.1600-0633.2010.00418.x.

Kottek, M., Grieser, J., Beck, C., Rudolf, B., and Rubel, F., 2006, World map of the Köppen-Geiger climate classification updated: Meteorologische Zeitschrift (Berlin), v. 15, no. 3, p. 259–263, accessed January 9, 2021, at https://doi.org/10.1127/0941-2948/2006/0130.

Lowney, C.L., 2000, Stream temperature variation in regulated rivers–Evidence for a spatial pattern in daily minimum and maximum magnitudes: Water Resources Research, v. 36, no. 10, p. 2947–2955, accessed January 13, 2021, at https://doi.org/10.1029/2000WR900142.

McCullough, D.A., 1999, A review and synthesis of effects of alterations to the water temperature regime on freshwater life stages of salmonids, with special reference to Chinook salmon, EPA 910-R-99-010, 279 p., accessed January 13, 2021, at http://wvvvv.krisweb.com/biblio/gen_usepa_mccullough_1999.pdf.

National Marine Fisheries Service, 2008, Willamette Basin Biological Opinion—Endangered Species Act Section 7(a)(2) Consultation: National Oceanic and Atmospheric Administration Fisheries Log Number F/NWR/2000/02117, [variously paged], accessed November 30, 2020, at https://www.fisheries.noaa.gov/resource/document/consultation-willamette-river-basin-flood-control-project.

NOAA National Centers for Environmental Information, 2020, Climate at a glance: Divisional Time Series, accessed December 7, 2020, at https://www.ncdc.noaa.gov/cag/.

Olden, J.D., and Naiman, R.J., 2010, Incorporating thermal regimes into environmental flows assessments—Modifying dam operations to restore freshwater ecosystem integrity: Freshwater Biology, v. 55, no. 1, p. 86–107, accessed January 13, 2021, at https://doi.org/10.1111/j.1365-2427.2009.02179.x.

Oregon Department of Environmental Quality, 2003, Figure 340A—Fish use designations—Willamette Basin, Oregon: State of Oregon Department of Environmental Quality map, accessed December 13, 2020, at https://www.oregon.gov/deq/FilterRulemakingDocs/figure340a.pdf.

Oregon Department of Environmental Quality, 2005, Figure 340B—Salmon and steelhead spawning use designations, Willamette Basin, Oregon: State of Oregon Department of Environmental Quality map, accessed December 13, 2020, at https://www.oregon.gov/deq/FilterRulemakingDocs/figure340b.pdf.

Oregon Department of Environmental Quality, 2006, Willamette Basin total maximum daily load program documents: Oregon Department of Environmental Quality, accessed January 5, 2021, at https://www.oregon.gov/deq/wq/tmdls/Pages/TMDLs-Willamette-Basin.aspx.

Oregon Department of Environmental Quality, 2016, Water quality standards—Beneficial uses, policies, and criteria for Oregon—Temperature: Oregon Administrative Rule 340–041–0028(4): Oregon Department of Environmental Quality, accessed December 13, 2020, at https://secure.sos.state.or.us/oard/viewSingleRule.action?ruleVrsnRsn=244176

Oregon Department of Fish and Wildlife, and National Marine Fisheries Service, 2011, Upper Willamette River Conservation & Recovery Plan for Chinook Salmon & Steelhead, Oregon Department of Fish and Wildlife, [variously paged], accessed December 13, 2020, at https://www.dfw.state.or.us/fish/crp/upper_willamette_river_plan.asp.

Palmer, R.W., and O'Keeffe, J.H., 1989, Temperature characteristics of an impounded river: Archiv für Hydrobiologie, v. 116, p. 471–485.

Perry, R.W., Plumb, J.M., and Huntington, C.W., 2015, Using a laboratory-based growth model to estimate mass- and temperature-dependent growth parameters across population of juvenile Chinook salmon: Transactions of the American Fisheries Society, v. 144, p. 331–336, accessed January 13, 2021, at https://doi.org/10.1080/00028487.2014.996667.

Preece, R.M., and Jones, H.A., 2002, The effect of Keepit Dam on the temperature regime of the Namoi River, Australia: River Research and Applications, v. 18, no. 4, p. 397–414, accessed January 13, 2021, at https://doi.org/10.1002/rra.686.

Rounds, S.A., 2007, Temperature effects of point sources, riparian shading, and dam operations on the Willamette River, Oregon: U.S. Geological Survey Scientific Investigations Report 2007–5185, 34 p. [Also available at https://doi.org/10.3133/sir20075185.]

Rounds, S.A., 2010, Thermal effects of dams in the Willamette River Basin, Oregon: U.S. Geological Survey Scientific Investigations Report 2010–5153, 64 p. [Also available at https://doi.org/10.3133/sir20105153.]

Rounds, S.A., and Buccola, N.L., 2015, Improved algorithms in the CE–QUAL–W2 water-quality model for blending dam releases to meet downstream water-temperature targets: U.S. Geological Survey Open-File Report 2015–1027, 36 p. [Also available at https://doi.org/10.3133/ofr20151027.]

Sinokrot, B.A., and Stefan, H.G., 1993, Stream temperature dynamics—Measurements and modeling: Water Resources Research, v. 29, no. 7, p. 2299–2312, accessed January 5, 2021, at https://doi.org/10.1029/93WR00540.

Steel, E.A., and Lange, I.A., 2007, Using wavelet analysis to detect changes in water temperature regimes at multiple scales—Effects of multi-purpose dams in the Willamette River Basin: River Research and Applications, v. 23, no. 4, p. 351–359, accessed January 13, 2021, at https://doi.org/10.1002/rra.985.

Stevens, L.E., Shannon, J.P., and Blinn, D.W., 1997, Colorado River benthic ecology in Grand Canyon, Arizona, USA—Dam, tributary and geomorphological influences: Regulated Rivers, v. 13, no. 2, p. 129–149, accessed January 13, 2021, at https://doi.org/10.1002/(SICI)1099-1646(199703)13:2%3C129::AID-RRR431%3E3.0.CO;2-S.

Stratton Garvin, L.E., and Rounds, S.A., 2022a, The thermal landscape of the Willamette River—Patterns and controls on stream temperature and implications for flow management and cold-water salmonids: U.S. Geological Survey Scientific Investigations Report 2022–5035, 43 p. [Also available at https://doi.org/10.3133/sir20225035.]

Stratton Garvin, L.E., and Rounds, S.A., 2022b, CE-QUAL-W2 models for the Willamette River and major tributaries below U.S. Army Corps of Engineers dams—2011, 2015, and 2016: U.S. Geological Survey data release, https://doi.org/10.5066/P908DXKH.

Stratton Garvin, L.E., Rounds, S.A., and Buccola, N.L., 2022a, Updates to models of streamflow and water temperature for 2011, 2015, and 2016 in rivers of the Willamette River Basin, Oregon: U.S. Geological Survey Open-File Report 2022–1017, 73 p. [Also available at https://doi.org/10.3133/ofr20221017.]

Stratton Garvin, L.E., Rounds, S.A., and Buccola, N.L., 2022b, Estimating stream temperature in the Willamette River Basin, northwestern Oregon—A regression-based approach: U.S. Geological Survey Scientific Investigations Report 2021–5022, 40 p. [Also available at https://doi.org/10.3133/sir20215022.]

Sullivan, A.B., and Rounds, S.A., 2004, Modeling streamflow and water temperature in the North Santiam and Santiam Rivers, Oregon, 2001–02: U.S. Geological Survey Scientific Investigations Report 2004–5001, 35 p. [Also available at https://doi.org/10.3133/sir20045001.]

Sullivan, A.B., Rounds, S.A., Sobieszczyk, S., and Bragg, H.M., 2007, Modeling hydrodynamics, water temperature, and suspended sediment in Detroit Lake, Oregon: U.S. Geological Survey Scientific Investigations Report 2007–5008, 40 p. [Also available at https://doi.org/10.3133/sir20075008.]

U.S. Army Corps of Engineers, 2019, Willamette Basin Review feasibility study—Final integrated feasibility report and environmental assessment: Portland, Oregon, U.S. Army Corps of Engineers, Portland District, 165 p., accessed May 5, 2020, at https://usace.contentdm.oclc.org/utils/getfile/collection/p16021coll7/id/13273.

Ward, J.V., 1985, Thermal characteristics of running waters: Hydrobiologia, v. 125, no. 1, p. 31–46, accessed January 13, 2021, at https://doi.org/10.1007/BF00045924.

Wells, S.A., 2019, CE-QUAL-W2—A two-dimensional, laterally averaged, hydrodynamic and water-quality model, version 4.2 user manual: Portland, Oregon, Portland State University, Department of Civil and Environmental Engineering, [variously paged].

Appendix 1. Changes to the CE-QUAL-W2 Control File

The CE-QUAL-W2 control file (w2_con.npt) was modified in this study to allow for better control over specialized output files, and to modify the capabilities related to generic constituents. The time-series output section was modified so that it now looks like:

```
TSR PLOT    TSRC    NTSR   NITSR  SPSRFC  SPVOLC  SPFLOC  HFLUXC
              ON       2      18     OFF   DAILY     OFF      ON
```

where the last four inputs are new, and replace a single SPTEMPC input that was removed. The SPSRFC input controls the creation of special surface layer output files. The SPVOLC input controls the creation of special volume-averaged output files. The SPFLOC input controls the creation of special flow-averaged output files, and the HFLUXC input controls the creation of a special heat-flux output file. The recognized values for these inputs are as follows:

Value	SPSRFC	SPVOLC	SPFLOC	HFLUXC
' ON'	Daily and subdaily outputs (SurfTemp.dat and SurfTemp2.dat)	Daily and subdaily outputs (VolTemp.dat and VolTemp2.dat)	Daily and subdaily outputs (FlowTemp.dat and FlowTemp2.dat)	Daily output (HeatFluxes.csv)
' DAILY'	Daily output only (SurfTemp.dat)	Daily output only (VolTemp.dat)	Daily output only (FlowTemp.dat)	No output
' SUBD'	Subdaily output only (SurfTemp2.dat)	Subdaily output only (VolTemp2.dat)	Subdaily output only (FlowTemp2.dat)	No output
anything else	No output	No output	No output	No output

The *Temp.dat output files include daily maximum, mean, and minimum water temperature as well as daily mean water-quality concentrations for every segment in the model domain and for every day of the simulation. The *Temp2.dat output files contain subdaily model outputs for temperature and the water-quality concentrations for every segment in the model domain and for every day of the simulation. Tracked heat components in the *Temp.dat and *Temp2.dat files are converted to percentages, and tracked ages are converted to time in days for output. The HeatFluxes.csv file contains specialized heat flux calculations and several time scales and ratios that may be helpful for determining the sensitivity of downstream temperatures to upstream flow and heat sources; more information on the HeatFluxes.csv file is provided in appendix 3.

The generic constituent rates section of the control file was modified to add two new inputs, relative to the unmodified release version of CE-QUAL-W2, as follows:

```
GENERIC    CGQ10   CG0DK   CG1DK     CGS   CGLDK   CGKLF    CGCS  CGTYPE   CGSRC
AGE         0.00   -1.00    0.00    0.00    0.00    0.00    0.00     AGE      NA
QT_DAMS     0.00    0.00    0.00    0.00    0.00    0.00    0.00 QTRACER      NA
HT_INIT     0.00    0.00    0.00    0.00    0.00    0.00    0.00 HT_INIT      NA
HT_DAMS     0.00    0.00    0.00    0.00    0.00    0.00    0.00  HT_INP      NA
HT_INP      0.00    0.00    0.00    0.00    0.00    0.00    0.00  HT_INP      NA
HT_EXCH     0.00    0.00    0.00    0.00    0.00    0.00    0.00 HT_EXCH      NA
HT_AGE      0.00   -1.00    0.00    0.00    0.00    0.00    0.00  HT_AGE      NA
AQ_DAMS     0.00   -1.00    0.00    0.00    0.00    0.00    0.00 AGE_SRC QT_DAMS
AH_DAMS     0.00   -1.00    0.00    0.00    0.00    0.00    0.00 AGE_SRC HT_DAMS
```

The CGTYPE and CGSRC inputs are the new input variables. The CGTYPE variable must be right-justified, and is used to specify the type of generic constituent. The CGSRC variable is used to specify the name of the generic constituent whose age is tracked by another generic constituent. The CG0DK input is set to -1.0 for constituents tracking age. Recognized values of CGTYPE are as follows:

Value	CGTYPE
' AGE'	Used to track the average age of water; needed to properly handle evaporation
' QTRACER'	Used to track fraction of water from an identified source; needed to properly handle evaporation
' HT_INIT'	Used to track the heat content tied to initial conditions
' HT_INP'	Used to track heat from an identified water source
' HT_EXCH'	Used to track heat from environmental energy fluxes across air/water, sediment/water interfaces
' HT_AGE'	Used to track the average age of heat
' AGE_SRC'	Used to track the average age of another generic constituent that is identified by CGSRC input
anything else	No special meaning; no tracking of water source, heat source, or age

The only generic constituents that can be age-tracked by specifying a CGTYPE of ' AGE_SRC' are those that have a CGTYPE of ' QTRACER', ' HT_INIT', ' HT_INP', and ' HT_EXCH'. The generic constituent name given as the CGSRC input must match the actual short name of the constituent given in the list of active constituents (CST ACTIVE card) in the control file.

Appendix 2. Changes to CE-QUAL-W2 Source Code

The final modified CE-QUAL-W2 source code and compiled model program used in this study are available online in a package posted on Science Base at https://doi.org/10.5066/P908DXKH (Stratton Garvin and Rounds, 2022b). The code used in this study is based on version 4.2 of the model as released by Portland State University on September 20, 2019. It is neither efficient nor particularly useful to post all of the code changes in this document, but all changes are marked in the source code with comments that include the author's initials and the date (MM/DD/YY), such as "!SR 03/14/20." The program was compiled with the Intel Visual Fortran compiler, version 12.0.4.196 and dated April 27, 2011. The options used to compile each source file are documented in a batch file that is included in the source-code package.

Here is a summary of the most-important or most-noticeable changes to the model source code as implemented in this study:

- The source code used in this study was a version with a "generic" text-based interface; all of the code for the graphical user interface was removed.
- Specialized code was added to track the water, heat, age of water, and age of heat from identified sources, as discussed in this report.
- Specialized and optional output files for daily and subdaily temperature and water-quality results were added, with code changes primarily in the outputinitw2tools.f90 and outputa2w2tools.f90 source files.
- A new HeatFluxes.csv optional output file was added to report various energy fluxes, time scales, and ratios, with code changes primarily in the outputinitw2tools.f90 and outputa2w2tools.f90 source files.
- Upgrades were made to the simultaneous model-run capability, such that downstream models that require input from the output of upstream models can be run concurrently with those upstream models. The downstream models will wait for output from the upstream models, run as far as they can, and wait for more output until they can complete their runs. The original code from Portland State University implemented this simultaneous capability with heavy use of the restart option; changes were made to avoid the restart option and use new code primarily in the TIME_VARYING_DATA subroutines. The awaited files need not exist at the beginning of a model run, so that all simultaneous models can be started at the same time.
- The "W2Errordump.opt" output file, which is produced if/when the model fails, was reorganized and reformatted as a csv file ("W2Errordump.csv").
- Custom USGS-based code was carried forward from previous versions, including (1) code to fix the phosphorus sorption algorithms, (2) code to fix the silica sorption algorithms, (3) code to fix problems with the settling fluxes of inorganic suspended sediments, and (4) code to allow pH as a boundary condition instead of total inorganic carbon. More information on the fixes to the sorption code are provided in a document included with the source-code package.

Appendix 3. The HeatFluxes.csv Output File

A new “HeatFluxes.csv” output file was added to the CE-QUAL-W2 model. The user activates this output option by setting the HFLUXC input to “ ON” on the time-series “TSR PLOT” input card in the control file. Heat calculations must be turned on in the model (HEATC set to “ ON”) in at least one waterbody for this output file to be created and for the specialized computations to occur. The output file includes results for each day of a model simulation and for every model segment in the waterbodies where heat calculations are turned on, as follows:

```
#Daily energy fluxes and daily mean energy ratios based on subdaily ratios
#  SEG  = model segment
#  HF   = heat flux
#  EEF  = environmental energy flux across air/water interface
#  HRTS = Heat replacement time scale (days):  ratio of heat content to incoming EEF
#  ADER = Advective HF to EEF ratio:  ratio of advective HF to incoming EEF
#  EEFR = EEF ratio:  ratio of total incoming EEF to total outgoing EEF
#  EEFN = daily net EEF (incoming total minus outgoing total; gJ)
#  EFLW = total daily energy gain due to long-wave radiation (gJ)
#  EFSW = total daily energy gain due to short-wave radiation (gJ)
#  EFCI = total daily energy gain due to conduction (gJ)
#  EFCO = total daily energy loss due to conduction (gJ)
#  EFBR = total daily energy loss due to back-radiation (gJ)
#  EFEO = total daily energy loss due to evaporation (gJ)
#  EFEI = total daily energy gain due to condensation (gJ)
#  SHAD = Daily mean shade factor for daylight hours
#  WTDR = Daily mean surface width to mean depth ratio
#  MWID = Daily mean surface width
#
JDAY,SEG,HRTS,ADER,EEFR,EEFN,EFLW,EFSW,EFCI,EFCO,EFBR,EFEO,EFEI,SHAD,WTDR,MWID
80,2,1.5008,335.7160,1.2844,85.8413,221.4763,130.1135,15.4322,.5015,263.5696,17.1310,.0214,.9911,34.1684,43.694
80,3,1.6242,335.9999,1.2813,85.1500,221.4763,129.6530,15.3537,.4971,263.6282,17.2290,.0214,.9876,31.6460,43.823
80,4,1.7200,365.3619,1.2463,82.0396,228.7441,126.5519,16.4313,.4828,271.5176,17.7111,.0239,.9050,31.4995,45.150
80,5,1.6195,341.0962,1.2106,70.9905,244.3858,119.3837,17.1474,.5224,290.7134,18.7174,.0267,.8241,35.8146,48.236
80,6,1.6370,333.3252,1.1853,64.2052,251.0612,113.8649,17.6216,.5287,298.6772,19.1802,.0436,.7669,36.5843,49.671
```

In that output file, JDAY is the day of the simulation, and in this case typically was set such that day 1.0 is the start of the day on January 1. The energy fluxes typically are expressed in gigaJoules (gJ), and the daily mean surface width is in meters. The heat replacement time scale (HRTS) is computed as the total heat content in the model segment, relative to liquid water at 0.0 °C, divided by the total incoming environmental energy flux, and has units of days. The advective heat flux is computed as the sum of the horizontal advective heat fluxes at the downstream boundary of each cell in a model segment; the ratio of the advective heat flux to the total incoming environmental energy flux (ADER) is dimensionless. The daily mean surface width (MWID), the daily mean surface-width-to-mean-depth ratio (WTDR), the daily mean heat replacement time scale (HRTS), the daily mean ratio of the advective heat flux to the incoming environmental energy flux (ADER), and the ratio of the incoming to outgoing environmental energy fluxes (EEFR) are computed as simple counted means for the day, for every instance when time-series output was requested (example: TSRF=0.025 means 40 times per day), with midnight belonging to the following day.

The total daily energy gains and losses are reported as integrated and interpolated sums over the course of the day, with integration using the trapezoidal rule. The daily net environmental energy flux (EEFN) is based on the reported daily sums of energy fluxes, and includes only those energy fluxes occurring across the air/water interface. The incoming and outgoing conductive energy fluxes also are reported only for those occurring across the air/water interface. The daily mean shade factor is computed as the sum of the shaded short-wave solar energy flux over the entire day, divided by the sum of the unshaded short-wave solar energy flux over the entire day, such that a factor of 1.000 means no shading and a factor of 0.500 means that half of the short-wave solar radiation over the course of the day was blocked by topographic or vegetative shade.

Publishing support provided by the U.S. Geological Survey
Science Publishing Network, Tacoma Publishing Service Center
For more information concerning the research in this report, contact the
Director, Oregon Water Science Center
U.S. Geological Survey
2130 SW 5th Avenue
Portland, Oregon 97201
https://www.usgs.gov/centers/or-water

ISSN 2328-0328 (online)
https://doi.org/10.3133/sir20225006